

PROPERTY OF
ARGONNE NATIONAL LAB
ID 4412 LIBRARY

THE MARK-II INTEGRAL SODIUM TREAT LOOP

L. E. Robinson, R. T. Purviance,
and K. J. Schmidt



U of C-AUA-USAEC

ARGONNE NATIONAL LABORATORY, ARGONNE, ILLINOIS

Prepared for the U.S. ATOMIC ENERGY COMMISSION
under contract W-31-109-Eng-38

The facilities of Argonne National Laboratory are owned by the United States Government. Under the terms of a contract (W-31-109-Eng-38) between the U. S. Atomic Energy Commission, Argonne Universities Association and The University of Chicago, the University employs the staff and operates the Laboratory in accordance with policies and programs formulated, approved and reviewed by the Association.

MEMBERS OF ARGONNE UNIVERSITIES ASSOCIATION

The University of Arizona	Kansas State University	The Ohio State University
Carnegie-Mellon University	The University of Kansas	Ohio University
Case Western Reserve University	Loyola University	The Pennsylvania State University
The University of Chicago	Marquette University	Purdue University
University of Cincinnati	Michigan State University	Saint Louis University
Illinois Institute of Technology	The University of Michigan	Southern Illinois University
University of Illinois	University of Minnesota	The University of Texas at Austin
Indiana University	University of Missouri	Washington University
Iowa State University	Northwestern University	Wayne State University
The University of Iowa	University of Notre Dame	The University of Wisconsin

NOTICE

This report was prepared as an account of work sponsored by the United States Government. Neither the United States nor the United States Atomic Energy Commission, nor any of their employees, nor any of their contractors, subcontractors, or their employees, makes any warranty, express or implied, or assumes any legal liability or responsibility for the accuracy, completeness or usefulness of any information, apparatus, product or process disclosed, or represents that its use would not infringe privately-owned rights.

Printed in the United States of America
Available from
National Technical Information Service
U.S. Department of Commerce
5285 Port Royal Road
Springfield, Virginia 22151
Price: Printed Copy \$3.00; Microfiche \$0.95

ARGONNE NATIONAL LABORATORY
9700 South Cass Avenue
Argonne, Illinois 60439

THE MARK-II INTEGRAL SODIUM TREAT LOOP

by

L. E. Robinson, R. T. Purviance,
and K. J. Schmidt

Reactor Analysis and Safety Division

November 1971

TABLE OF CONTENTS

	<u>Page</u>
ABSTRACT	5
I. INTRODUCTION	5
II. DESIGN CONSIDERATIONS	6
A. Criteria	6
B. Conceptual Design	7
C. Engineering Design Considerations	9
D. Selection of the Sodium Pump	13
E. Flanges	16
F. Design Stresses	17
G. Stress Analysis	18
1. General Discussion	18
2. Discussion of Steady-state Pressure Capabilities	19
III. DESIGN DESCRIPTION OF THE MARK-II LOOP	23
A. Loop	23
B. Loop Instrumentation and Control	27
IV. QUALITY STANDARDS, CONTROL, AND ASSURANCE	28
A. Quality Levels	28
B. Quality Control and Assurance	30
V. PROTOTYPE LOOP TESTING	37
APPENDIXES	
A. Proof test Form for the Mark-II Integral Loop	41
B. Detailed Stress Analysis for the Mark-II Loop	43
REFERENCES	66

LIST OF FIGURES

<u>No.</u>	<u>Title</u>	<u>Page</u>
1.	Isometric Drawing of ALIP.	15
2.	ALIP Flange and C-type Autoclave Clamps	17
3.	Line-drawing Layout of the Mark-II Integral Sodium TREAT Loop	23
4.	Mark-II Loop Assembly before Outfitting	24
5.	Finished Mark-IIA Loop next to Loop Containment Can	26
6.	Flow Diagram of Mark-II Loop Development	31
7.	Diagram of Loop Documentation	31
B.1.	Piping Schematic Diagram.	55

TABLE

<u>No.</u>	<u>Title</u>	<u>Page</u>
I.	Values of Stress Intensity in the Principal Tubular Sections . .	20

THE MARK-II INTEGRAL SODIUM TREAT LOOP

by

L. E. Robinson, R. T. Purviance,
and K. J. Schmidt

ABSTRACT

Performance of Fast Reactor Safety experiments in which oxide fuel is melted and failed in the presence of sodium coolant requires special test techniques. This report describes the engineering criteria, design, fabrication, and prototype testing of the Mark-II Integral Sodium Loops developed for studying LMFBR oxide-fuel behavior under transient testing to failure in the TREAT reactor. The basic design point is a rating of 5000 psi at 1000°F.

I. INTRODUCTION

This report describes the basic development of a second-generation integral sodium loop for advanced meltdown experiments in TREAT. The advanced loop with more extensive instrumentation, a larger test section, and higher operating temperature and pressure, was designed on the basis of experience gained with the Mark-I TREAT Integral Sodium Loop. Remote and semiremote handling capabilities for use with plutonium-bearing specimens were also considered in the advanced loop or "Mark-II" design.

The Mark-I loop^{1,2} was intended for experimental use in TREAT meltdown experiments of relatively low-melting-point metallic fast reactor fuels contained in flowing sodium. These loops have been used successfully and routinely for such tests. However, the design pressure of 30 atm at 500°C and steady-state temperature limitation below 400°C are not adequate for LMFBR oxide-fuel transient safety experiments. The counterflow design of the Mark-I loop was required to reduce the loop size to fit within a single TREAT fuel-element can. However, this counterflow feature made the instrumentation of pressure, flow, and temperature difficult.

Covered in this report is the work leading up to the use of the Mark-IIA advanced loops. Other possible variations of the basic Mark-II type are not included. Variations in the Mark-II loop made to date are described later.

II. DESIGN CONSIDERATIONS

A. Criteria

Experience gained from the use of the Mark-I loop in TREAT clarified the requirements for the Mark-II integral sodium loop.

The Mark-II loop must contain the high-amplitude pressure pulses which might be generated by the failure of refractory fuel elements with melting points well above 2000°C. The loop in its entirety would be required to function properly under steady-state conditions at the operating temperatures typical of fast power reactors. The flow of sodium in the Mark-II loop should be adequate to simulate thermalhydraulic conditions in typical LMFBR oxide-fueled designs, and the pump and its controls would require sufficient latitude and versatility to permit experiments with flow decay.

In experimental use, the advanced loop should offer increased ease of fuel loading and unloading, whether the operations are performed on the laboratory work bench or within an α -cave. Hence, the loop should be capable of being easily filled with sodium and easily drained by remote means.* The test section should be capable of having a single oxide fuel element as well as a three-row cluster of 19 pins of the EBR-II driver type. Sample-length capabilities should be sufficient to accommodate the longest pins under irradiation in EBR-II.

The primary containment of the loop body should have an expansion chamber as a safety measure. The expansion chamber and any necessary connecting lines must have sufficient pressure capability and containment integrity that venting would not compromise loop integrity.

Secondary containment of the loop system should be provided, as in the case of the Mark-I loop, by suitable enclosure within a hermetically sealed stainless steel TREAT dummy element containing an inert atmosphere.

The justification for the design and construction of experimental apparatus is the acquisition of data. The fuel-holding leg of the Mark-II loop should be fully instrumented at inlet and outlet to measure sodium pressure, flow rate, and temperature accurately. The sensors should be as unresponsive to the extreme nuclear radiation of the reactor as is feasible.

There should be capability to permit use of instrumented fuel or (more generally) to adjust instrumentation leads into the loop. For proper operation, the temperature of the sodium and of heat-limited loop components would be continually monitored. *

*At least until sufficient experience was gained in loop operations to show that this capability was not in fact needed.

B. Conceptual Design

The requirements listed above were fulfilled in the conceptual design of the Mark-II integral sodium TREAT loop.

Requirements of a larger test section and higher pressure rating over the Mark-I loop made it impossible to keep the volume required for enclosure of the advanced loop within that available in a single TREAT fuel element can. Housing the loop complex in a shell having the size of two TREAT fuel elements also made possible a simplification of the loop structure.

The 8-ft vertical length and 4 x 8-in. cross section of two elements could accommodate an elongated miniature loop of two straight parallel legs, the downcomer in one side and the riser test section in the other side of the shell. Access to the fuel-containing test section could be provided by adding an extension beyond the return bend of the loop and on the centerline of the test section. With a liquid-metal pump in the downcomer leg, a closed-circuit, direct-flow recirculating system was feasible. The extension also provided a plenum for expansion volume. The simplified geometry offered the immediate advantage of providing the fast-neutron hodoscope with a relatively uncluttered view of the fuel-containing test section, while the loop is positioned in the reactor with the test section leg in the hodoscope viewing slot. The direct straight-through sodium flow would result in lower hydraulic losses, and assure greater ease in instrumenting both the inlet and outlet of the fueled test section, while facilitating the assembly and disassembly of successive experiments by remote handling.

With a test section of sufficient length to accommodate a test fuel pin of about 76 cm (30 in.),* centered on the horizontal centerline of the TREAT core, there was approximately 50 cm of space left between the bottom of the secondary enclosure can and the lower bend of the loop to provide for a safety expansion tank. This tank is connected to the loop by a vent line closed by a calibrated burst-disc pressure-relief valve.

Some of the problems encountered in the experimental utilization of the Mark-I integral loop could be assuaged by design of the safety tank to serve also as a dump tank which would provide volume for storage of the loop liquid sodium as well as vented overpressure expansion of sodium vapor. In combination with the multipurpose "safety" tank, the installation of a valved fill/drain line into the bottom of the advanced loop, a valved overflow line between the desired level of sodium in the loop and the tank, and an externally supplied helium pressure line into the tank, was conceived as a technique to assure a fixed sodium level within the loop, without the necessity of probing, and by a completely remote operation.

*Sufficient to accommodate the longest pins under irradiation in EBR-II at that time.

The operational valving for the fill/drain and the overflow lines was envisioned as a combination of commercially available mechanical valves and the long-used sodium freeze valve, since the auxiliary connecting lines and valves should permit the intermittent flow and shutoff of molten sodium, while possessing the same pressure capability as the loop proper during transient experimental operation.

The feasibility of the conceptual design of the Mark-II integral loop geometry depended primarily on the availability of a liquid-metal pump which could meet the operational requirements of the advanced facility. The requirements placing the most stringent demands on the sodium pump were the design pressure capability greater by an order of magnitude than that of the first generation of integral loops, a steady-state pumped-sodium design temperature of about the same level ($\sim 500^\circ\text{C}$), and the severe size limitation which required the finished loop to fit into a rectangular cross section of 4 x 8 in. (10.16 x 20.3 cm). Other capabilities involving operational parameters were considered desirable (within limits), but not absolutely necessary, for the experimental usability of the integral loop. These factors included a high flow capability (8 m/sec optimum), a programmable flow rate, reversibility of flow direction, ease of replacement in the event of failure, reasonable efficiency, and versatility of pumping performance to meet a wide range of experimental requirements.

The combination of pressure, containment, and temperature criteria eliminated the Faraday-conduction-type electromagnetic pumps, which characteristically require very thin walls for operation at measurable efficiencies, and most of the mechanically rotatable field pumps, which rely on close coupling of a permanent magnetic field with the conductive liquid metal being pumped. The size limitation effectively eliminated the polyphase helical and the mechanical axicentrifugal types of pump.

The only sodium pumps previously developed which seemed to offer some possibility of adaptation to the proposed advanced loop were the Flat Linear Induction Pump (FLIP) and the Annular Linear Induction Pump (ALIP). Each is a polyphase traveling-wave electromagnetic liquid-metal pump, characterized by a geometry having a large ratio of length to diameter. The FLIP has been built in large-size versions and was routinely operated to transfer or circulate sodium and NaK in large volume flow systems, whereas only experimental versions of the ALIP had been built and operated, also in high flow-rate systems. However, the geometry and modes of operation of both types offered the possibility of miniaturization for use in the integral loop. The extra-loop location of the driving stator of the linear induction pumps would permit sufficient increase in the flow-channel walls to contain high internal pressures (however, at the expense of pump efficiency) while allowing fluid cooling of the stator coils and laminations to remove the heat generated from the electrical power losses and heat conducted from the hot loop sodium. The pump-design flow, efficiency, and capability

for varying characteristics would depend on the degree of degradation of pump properties accompanying drastic miniaturization.

Either type of pump could be replaced in the loop, provided that high-integrity, leak-free, high-pressure flanged connections could be applied in miniature to the loop. However, an identical problem of flange miniaturization also was presented by the requirement for replaceable attachment of pressure transducers to the proposed loop, as well as the sealing closure of the sample-loading access port. The flange closure having the greatest intrinsic strength, the smallest overall size, the highest mechanical advantage, and the tightest seal under extreme internal pressures was the ramp-backed gasket-sealed flange, closed by split-C clamps, used for decades in the closures for autoclaves and reaction vessels. The "Conoseal" clamped flange connection is a proprietary version of the autoclave flange, using a deformable gasket, and has been used widely in sodium technology. A strengthened version, using the solid double-oval O-ring seal in routine use for ANL fast reactor safety tests, would not require the extreme flange travel required by the Conoseal version, and would permit the in-line installation of the sodium pump into the downcomer leg of the loop opposite the test section.

C. Engineering Design Considerations

The selection of the design point for the advanced integral sodium loop was admittedly arbitrary, since no data were available as to what pressure-time loadings would be encountered in the performance of the desired meltdown experiments using the refractory fast reactor fuel types. In fact, one reason for performing the experiments is to obtain experimental data on the pressure loading and molten-fuel movement. The Mark-I integral loop was designed for a rating of approximately 30-atm (450 psig) internal pressure at 500°C. The performance of meltdown experiments using ceramic fuels in the presence of sodium coolant required the selection of a pressure design point that was greater by an order of magnitude than the rating of the Mark-I loop at essentially the same initial temperature.

Thus, the design rating was taken to be an internal pressure of 340 atm (5000 psig) at a steady-state temperature of 538°C (1000°F). This design point requires a proof test pressure of 6250 psi, which is approximately the critical pressure of sodium.

In light of the uncertainty in the maximum amplitude of the forces to be contained during the proposed experiments, it was believed desirable to design the advanced loop in accordance with the most conservative code and rigorous standards applicable. Selection of the reference design code required the classification of the facility in terms of its intended use. The conceptual closed-loop flow-circuit geometry could be considered as a high-pressure, high-temperature piping system. However, the system was to

contain flowing sodium, and reactor fuel, and would effectively become a part of an operational nuclear reactor during an experiment. The loop would function as a free-surface vessel with a top penetration for loading and removing test samples, and a mechanical closure, as opposed to a permanently joined, fully filled welded piping system. Hence, it was deemed particularly suitable to base the design upon the well-established standards and specifications of the ASME Boiler and Pressure Vessel Code, 1965 edition.³ The conservatism of the ASME Code, with its 4-to-1 margin of ultimate tensile stress to rated (allowable) tensile stress, was an added incentive to use this Code as a base for the design. Thus, design calculations were based on the ASME Code, Section III, with the loop defined as a Class A Nuclear Vessel. Exceptions were taken toward even greater rigor.

Although the Mark-II loop was basically designed in accordance with the standards and specifications of the ASME Code,^{3,4} some exceptions and refinements were taken. The finished loops include a section of Inconel, which is not a Code-qualified material.* The standards established for the choice of materials, fabrication, inspection procedures and criteria, and the specifications of heat treatments, in most cases, reflect refinements of the Code standards.

The highest-strength Code-rated material at the design temperature, and of ready availability, and having full compatibility with molten sodium and high weldability, is Type 316 stainless steel. The Mark-II loop body, piping, hydraulic attachments, and accessory components are made wholly of Type 316 stainless steel, carefully selected by chemical composition, form, and thermal history. This is the standard T316 stainless steel, molybdenum stabilized; it offers the following advantages:

1. High strength at high temperatures.
2. Normally insensitive to notching.
3. Optional postweld heat treatment.
4. Readily machinable.
5. High ductility in its fully annealed state.

Conversely, the material has a number of disadvantages which require meticulous care in selection, fabrication, and inspection of material for devices such as the Mark-II loop. These include:

1. Despite the molybdenum additive, a higher tendency to precipitate brittle carbides, especially near massive welds.

*Compare, however, Case 1344-1 interpretation of ASME Boiler and Pressure Vessel Code (approved by council March 14, 1966).

2. Rigid control of chemical composition of the parent metal and weld metal to avoid carbide precipitation.

3. Like all 300-series austenitic stainless steels, work hardening readily, necessitating frequent annealing and practical experience in machining.

For long-term service, as in large systems such as stationary power plants, the Type 316H stainless steel has been used extensively for high-temperature, high-pressure applications; however, the high carbon content often results in lower weldability and age-cracking of weld joints.

The 316H stainless steel corresponds to the Code material designated SA-376.

The Code material selected for the Mark-II integral loops was SA-312, TP316, taken from Table N-421 of Ref. 4. The complete specification for this material, as given in Section II, "Materials," of Ref. 4 is equivalent to the ASTM Specification A312-64. For the Mark-II loop, the material was to be seamless throughout.

Although the T316 material has often been used for service at temperatures in excess of 1000°F, the allowable design stress values (Table N-241) given by the ASME Code for any material are tabulated only to a maximum temperature of 800°F; allowable yield strengths are given to a temperature of 1000°F (Table N-424). Although a higher temperature than 800°F is desirable, and Code values "are being worked on," the 1968 edition of the ASME Code has the same limitations.

Examination of the design stress values given in Table N-241 indicates a higher allowable stress at 800°F for SA-312, T321 and T347 stainless steels than for the SA-312, TP316. However, correlation of these values with those given in Section I, "Power Boilers," Table PG-23.1, and Section VIII, "Unfired Pressure Vessels," Table UHA-23, permit a reasonable extrapolation of the Section III values for SA-312, T316 to a stress S_m of 14,000 psi at 1000°F, which is considerably higher than the equivalent stresses for the other two steels. In addition, there is a more favorable history of experience with TP316 welds than with T347.

The allowable stress values given in the Code tabulation for both the 1965 and 1968* editions are subject to footnoted conditions: (1) the SA-312, TP316 stainless steel must have a carbon content greater than 0.04%, and (2) the metal must be heat treated to a minimum temperature specified (1800°F in the 1965 edition, and 1900°F in the 1968 edition). The first

*The yield stress for SA-312, TP316 was increased in the 1969 winter addition to the 1968 edition.

condition is required for enhancement of the basic strength of the Type 316 stainless steel at temperatures well above ambient; the second condition assures that the metal exists in the fully austenized state in which it possesses the greatest toughness and ductility. Meeting the requirement of carbon content is but a matter of material selection in accordance with chemical composition; however, assuring complete austenization of a complex geometry consisting of a welded composite of massive parts presented some difficulty.

Of greater import than the conditions imposed on the use of the material selected was the fact that the specific Code-qualified stainless steel, the SA-312, TP316 Seamless Austenitic Pipe, could not be obtained in the dimensions required by the design except by the prohibitive expense and lead times associated with special mill orders. If the selected material could not be procured in the desired form, of seamless pipe, the fabrication of the tubular form from solid bar or rod of Type 316 stainless steel must be justified. The equivalence of the properties of the finished tubular product with those of the Code-qualified SA-312, Type 316 seamless austenitic pipe, selected as the basic design material for the Mark-II loop, would have to be established.

A form of Type 316 stainless steel was sought among available stock materials which would insure a grain orientation and internal structure closely similar to that of the SA-312 seamless pipe, resulting from the forming process of mandrel drawing. The desired orientation should be unidirectional, with a radial symmetry about a common axis in the direction of drawing or rolling. By this, rolled plate was eliminated because it lacks the required radial symmetry of grain orientation, since it is formed by single roll reduction. The seam-welded pipe might be usable although formed of thin plate, except for the existence of the closure weld seam.

By the same token, round solid bar stock possesses the similar structural characteristics and grain orientation as a seamless pipe, with similar radial symmetry, since it is formed through a reducing die, or multiple rolls, with successive deformations in the axial direction of rolling. The rectangular bar, formed by reduction through double rolls, also is closely similar to pipe in its internal structure. Bar stock formed by cutting rolled plate was, of course, not acceptable for the reasons given for rejection of plate stock.

Consideration of the ASME Code-listed material forms revealed that the only T316 stainless steel in solid bar form was a high-alloy forging stock specification. Forged material, it was believed, would have a grain structure and mixed orientation sufficiently unlike that of the desired seamless pipe so as to be questionable for use as a base material.

The base material for the loop-body weldment was selected from ASTM specifications for bar stock, with chemical composition and physical properties identical, but restricted in composition with respect to carbon and nickel elements to those of the ASME Code-qualified SA-312, TP316 austenitic seamless pipe. The bar specified for fabrication of the tubular components of the loop body was ASTM A276-64, T316 austenitic stainless steel. With the exception of the return tee of the loop and the upper and lower instrument sections, A276 SS was procured in round bar form; for the return tee and the upper and lower instrument sections, rectangular bar was used as the stock material.

Those portions of the loop complex which are required to contain the internal pressures of the loop-body weldment, but are not a part of the circulatory system (i.e., the interconnecting piping of the overflow, fill and blowout lines), were obtainable in standard sizes of seamless pipe. However, the desired nominal sizes ($1/4$ -, $3/8$ -, and $1/2$ -in., Schedule 80 IPS) covered by the specification of SA-312, TP316 seamless austenitic pipe were not readily available. Thus, again, it became necessary to find an alternative equivalent in chemical composition, physical properties, and allowable design stress among the ASTM specified materials which were available. The ASTM A269-64, T316 seamless austenitic pipe and tubing, selected for chemical and physical properties, was equivalent and more readily obtainable.

The detailed specifications of all materials used in the construction of the Mark-II loop were followed rigorously. It should be noted that the chromium, nickel, and molybdenum content of bar, plate, pipe, and weld filler wire is a single specification, but the carbon content of the weld filler wire differs from that of the parent materials. The base metals are required to have a carbon content of $0.04\% < C < 0.08\%$, whereas the weld wire is specified to contain $0.05\% \leq C \leq 0.07\%$. The differential in carbon content provides a mechanism tending to decrease the concentration of carbon in the weld zone and inhibit the precipitation of carbides.

D. Selection of the Sodium Pump

The sodium pump selected for the Mark-II loop was the direct-flow version of the Annular Linear Induction Pump (ALIP), which proved to be the only type of liquid-metal pump amenable to the degree of miniaturization required and capable of containing the design internal pressure of the loop. An attempt was made to obtain a compacted version of the FLIP commercially, but costs for development and for subsequent pumps would be much higher than actually incurred by the ALIP, for a FLIP which could not be cooled during operation of the loop.

The ALIP, as designed for the Mark-II loop, was a miniaturized and modified version of the experimental sodium pumps designed and built by

Blake.⁵ Blake's sodium pump was of 14-in. OD x 52-in. long, air-cooled, and with a capacity of 600-700 gpm of sodium at a temperature of 600°C in direct-flow geometry. A counterflow design of the ALIP was constructed and thoroughly tested by Cambillard and Schwab⁶ for use in the RAPSODIE reactor, although it was never used. Their pump was designed for counterflow, to permit convenient maintenance and replacement of stator coils, without breaking the sodium-flow system. The relatively low-pressure flow tube in the counterflow pump was constructed of Nimonic-80 superalloy, which was joined to the flow system by welding to Type 321 stainless steel, a feat which was accomplished with extreme difficulty.

The two versions of the ALIP are mentioned because of the variation in results of design calculations carried out for the essentially similar devices. Blake's calculations were based upon Maxwell's equations, the inlet and outlet halves of the pump being mirror images of each other. Such calculations indicated that the stator field coils should be systematically reduced in the number of turns, or graded downward, over both inlet and outlet poles, to counteract the effects of field fringing, excessive power loss, and heat generation. Cambillard and Schwab performed a zone-to-zone iterative calculation, which resulted in an optimization of pump performance by reduction of the coil windings over the inlet pole, and successively increasing the number of turns on the coils towards the pump outlet.

The development and the results of operational testing of the Mark-II ALIP have been reported elsewhere. The Mark-II ALIP has an outer diameter of $3\frac{1}{2}$ in., a stator armature 19-in. long, and an overall length between flanges of approximately $25\frac{1}{2}$ in. This miniature ALIP has four poles, with two coils per phase per pole, for a total of six coils per pole; the inlet pole coils are graded from the pump inlet by thirds (i.e., successive coil pairs have $1/3$, $2/3$, and the balance the full number of turns). Figure 1 is an isometric line drawing showing the ALIP for the Mark-II loop. The pump behaves essentially like an induction motor with a liquid rotor. The ALIP limit is a three-phase, 60-cycle, 230-V ac, 50-A/phase device. The pump is fitted with a central core of magnetically soft metal which defines an annulus 0.375-cm wide, through which the molten sodium is driven by the traveling magnetic wave.

The pump stator is assembled upon an evacuated, multilayered stainless steel Dewar heat barrier, which is concentric with the sodium-flow tube of fully age-hardened Inconel X-750 and serves as thermal insulation for the stator assembly against the loop heat. The stator's 24 pancake coils are wound of fully anodized aluminum acrylic-coated ribbon, 0.5-in. wide and 0.008-in. thick, held in place by 12 symmetrically positioned slotted magnetic field yokes in a spoke-like radial array. The stator yokes are assembled from 29 gauge (0.356 mm) 1%-silicon transformer iron laminations which are tightly riveted together. The 1%-silicon iron was chosen for its high curie point, resulting in some increase in core power loss. The

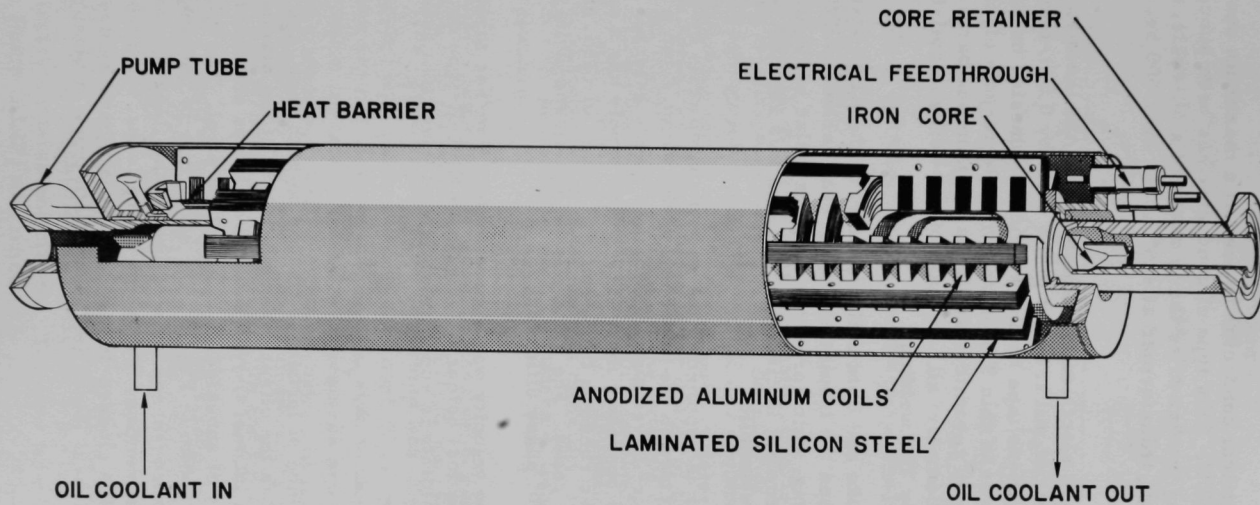


Fig. 1. Isometric Drawing of ALIP. ANL Neg. No. 112-8624.

anodized aluminum electrical conductor is used at a maximum operating temperature of about 260°C. This type of conductor has been successfully used without interleaving insulation as the primary of a 60-cycle, single-phase, 230-V ac stepdown transformer at 425°C, for over 500 hr, without malfunction.⁸

The field coils are electrically insulated from the laminated magnetic yokes by thin sheets of mica, bound to the coils by 0.051-mm-thick pressure-sensitive polyimide tape having a silicone adhesive backing, and by a circumferential layer of thin Teflon sheet. Pole-to-pole electrical connections are made with ceramic-insulated aluminum bus bars, of approximately 0.081-in. diameter; all internal coil-to-coil and coil-to-bus connections are made by TIG welding.

The magnetic yoke and field coil assembly of the ALIP stator is rigidly positioned between the insulating Dewar heat barrier and the stainless steel cooling housing, which provides a tight annular enclosure. Low-viscosity silicone oil* coolant is circulated through this annulus to cool the magnetic yoke in coil assemblies.

Electrical power is supplied to the sodium-pump coils by large-capacity through-connectors in the upper end of the pump, from a programmable three-phase, motor-driven autotransformer supply external to and at some distance from the operating loop. The power supply has a capacity of 60 A/phase, with a 5-sec rundown time from full power to zero, and an interlocking manual zero reset. The pump phases are closed-delta connected to ensure a constant 120° phase difference.

The desired flow velocity was approximately 9 m/sec through the test section containing a fuel holder filled with 19 EBR-II-type core fuel elements. This flow velocity is approximately equivalent to a flow rate of 110 liters/min.

E. Flanges

The ALIP flow tube of Inconel is flanged on both ends, and is clamped between mating flanges in the offset downcomer side of the stainless steel loop with age-hardened Inconel C-type autoclave clamps and solid double-oval O-ring flange seals of annealed T316 stainless steel. The ALIP-to-loop flange coupling is shown in Fig. 2. The same type of coupling is used to attach the loop pressure-sensor assemblies⁹ to the flanged pressure taps above and below the test section. For some of the loops, the access port at the top of the test-section closure-tube extension is closed by double-oval O-rings; on others Conoseal joints are used. Both types of closure have been used successfully.

*Dow 200 dimethylpolysiloxane, 20-centipoise viscosity.

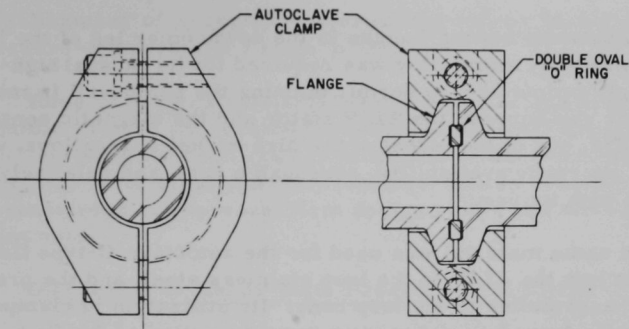


Fig. 2. ALIP Flange and C-type Autoclave Clamps. ANL Neg. No. 112-7429.

F. Design Stresses

Section III of the ASME Code requires all welds in the fabrication of a Class A Nuclear Vessel to be full penetration and certified as to quality by full radiographic examination. If this requirement is met throughout, a weld efficiency factor of 1.0 may be used in determining the maximum allowable stress value to be used in the design of the vessel. The massive scale of the Mark-II loop weldments, the extreme constriction of the loop interior dimensions, and the small-radius convolutions of its geometry are all factors which make full radiographic examination of completed welds difficult to achieve. As a result of this difficulty, the weld efficiency was derated by 10%, and a factor of 0.90, instead of unity, was adopted as an added precaution.

Hence, the allowable design stress value used for the T316 stainless steel of the loop structure was reduced from the Code-allowed 14,000 psi at 538°C (1000°F) to 12,600 psi. This value was used in the determination of the various wall thicknesses in the loop. This reduced value for allowable stress results in some overdesign, even in those portions of the loop complex which operate at design temperatures and provides a very large margin of containment safety in those regions of the system that always remain at relatively low operational temperatures (e.g., the closure-tube extension, safety/dump tank, and overflow and fill lines).

The reduction of allowable design stress, to ensure an additional margin of safety and the highest possible level of quality, constitutes a refinement to the design Code.

The major exception to the Code in the design of the Mark-II loop was the use of an unqualified material for a portion of the loop flow channel in the primary containment circuit. The flow tube of the Annular Linear Induction Pump (ALIP) was made of Inconel X-750, fully age-hardened, and

is clamped between mating flanges in the downcomer leg of the loop proper. Such a nonmagnetic superalloy was required for its unusual high-temperature, high-strength properties, to permit thinning the pump wall in minimizing the magnetic gap between the ALIP stator and the magnetic central core. Inconel X-750, one of the oldest of the high-nickel superalloys, was selected because of its ready availability, reasonable cost, and relatively extensive experience with its use.

The same material was used for the autoclave C-type flange clamps and bolts to join the ALIP to the loop stainless steel, and the pressure transducer assemblies to the loop body. Its utilization in clamps and bolts external to the loop does not constitute an exception to the Code.

Although the Inconel X-750 is not qualified by the ASME Code for pressure-vessel use,* the maximum allowable design stress for the material was calculated according to the most conservative method used in the determination of such stresses for qualified materials. As a further conservatism, the physical properties of wrought bar Inconel at 1000°F was used, instead of the much higher strengths of the fully age-hardened metal, as the base property for the calculation of design stress value. The Code prescribes that the lesser value obtained by calculating $62\frac{1}{2}\%$ of the yield strength at temperature, or determining 25% of the tensile strength, shall be taken to be the maximum allowable design stress of the subject material. The yield strength of Inconel X-750 is given as 84,000 psi and the tensile strength as 140,000 psi at the 1000°F design temperature of the Mark-II loop. The maximum allowable design stress of the Inconel used in the loop was taken to be 25% of the tensile strength at rated temperature, i.e., 35,000 psi. Derating of the finished pump by 10%, as with the loop proper, to an efficiency of 0.90, to account for possible weld efficiencies, resulted in an effective maximum allowable stress of 31,500 psi, which was used in the design of all Inconel components of the Mark-II loop. Thus, the Inconel pump wall thickness of 0.254 cm (0.100 in.) exceeds the exact design-thickness requirement for the 2.67-cm (1.050-in.) inner diameter by more than 16%.

A necessary consequence of using the Inconel was that stresses are produced by the differential thermal expansion between the pump flow tube and the stainless steel loop test section. This point will be considered in Section II.G and Appendix B.

G. Stress Analysis

1. General Discussion

The Mark-II integral sodium loop was designed, as described above, using the ASME Boiler and Pressure Vessel Code as a basis. Design calculations for the loop as a nuclear vessel were directed primarily

*Compare, however, Case 1344-1.

to the establishment of acceptable operational stress levels at the selected pressure-temperature design point.

Some scoping calculations were made in which estimates of the thermodynamic limit of conversion from sample thermal energy to work against the loop were checked against estimates of the containment capability of the loop for internal pressure loadings. These considerations could hardly be considered to represent firm design points and were performed for guidance only.

2. Discussion of Steady-state Pressure Capabilities

The Mark-II integral loop design is based on the 1965 edition of the ASME Code for Class A Nuclear Vessels for steady-state service of 5000 psi (340 atm) at 1000°F (538°C). The primary loop is comprised of components with circular cross section, in 4 different sizes. The test section has an outer diameter of 2 in., with a bore of 1.281 in.; the upper and lower bends have an OD of 1.250 in. and an ID of 0.750 in. The closure tube, or test-section loading extension tube, is larger than the test section for added convenience of access, having an OD of 2.250 in., and an ID of 1.469 in. The ALIP sodium pump has a thin-walled Inconel, annular flow section with an OD of 1.250 in. and an ID of 1.050 in.

The allowable design stress extrapolated from Section I, "Power Boilers," and Section VIII, "Unfired Pressure Vessels," for application to Section III, "Nuclear Vessels," was 14,000 psi at 1000°F for the SA-312, TP316 stainless steel. However, for this application the allowable design stress was derated to 12,600 psi for the following reasons. A 10% reduction in the design stress was taken to compensate for possible undetected flaws in the massive weldments. In addition, other factor-rated data provide increased assurance with respect to reliability of the loop to perform safely. The reduced design stress for the Inconel X-750 was taken to be $S_m = 31,500$ psi at 1000°F.

The allowable stress intensity is determined by the largest absolute value of the stress difference using averaged values of the membrane stresses. The stress differences are determined in accordance with Par. N-413 (e) of Section III of the Code. The equations are

$$S_{12} = \sigma_1 - \sigma_2; S_{23} = \sigma_2 - \sigma_3; S_{31} = \sigma_3 - \sigma_1.$$

The equations shown in Par. I-221 are used to calculate the component stresses:

$$\sigma_1 = \sigma_t = p[1 + (z^2/Y^2) - 1];$$

$$\sigma_2 = \sigma_\ell = p/(Y^2 - 1);$$

$$\sigma_3 = \sigma_r = p(1 - z^2)/(Y^2 - 1)$$

where p is the internal pressure in the tube (in psi), r_i the intermediate tube radius (in inches), r_1 the internal tube radius (in inches), r_2 the outside tube radius (in inches), and

$$Y = r_2/r_1;$$

$$Z = r_2/r_i.$$

The averaged membrane stress intensities are derived by averaging the stress components across the thickness of the tube section. To obtain the average stress component, the equations are solved for the stresses that occur at the inside surface of the tube and the outside surface, and then averaged arithmetically. Thus, the stress for the inside surface is found by using a value for Z equal to the ratio of r_2/r_1 , and the stress on the outside surface is found by using a value for Z equal to the ratio of $r_2/r_2 = 1$. The largest absolute value is given by S_{31} .

The results for the four principal tubular sections in the loop are shown in Table I. They range for the TP316 components from 12,500 psi for the closure tube to 10,690 psi for the bends, compared to an allowable stress value of 12,600 psi. The stress intensity for the Inconel X-750 ALIP tube was found to be 29,000 psi, compared to an allowable stress value of 31,500 psi.

TABLE I. Values of Stress Intensity in the Principal Tubular Sections

Component	r_1 , in.	r_i , in.	σ_{av} , psi	σ_{3av} , psi	$ \sigma_{31av} $, psi	Allowable Design Stress, psi
Closure Tube	0.735	1.125	10,000	-2500	12,500	12,600
Test Section	0.640	1.000	9,450	-2500	11,950	12,600
Bends	0.370	0.625	8,200	-2500	10,690	12,600
ALIP Tube	0.525	0.625	26,500	-2500	29,000	31,500

The 1969 Addenda to the 1968 Code notes an increase in the allowable yield strength in SA-312 TP316 SS tubular products from 15,700 to 17,000 psi at 1000°F. In accordance with Appendix II, Basis for Establishing Design Stress Values, the selection of 90% of the yield strength as the lowest of four criteria for calculating the design stress for austenitic steels gives a value of 15,300 psi. Derating this value by 10%, consistent with the practice followed in this design, gives 13,800 psi, a value about 10% higher than the 12,600 psi used in the design.

If the average tangential stresses are determined by integrating the stresses over the wall thickness rather than by arithmetically averaging the inside and outside values for the various wall thicknesses, the average values will be approximately 6-10% lower. Thus, the average integrated stress is found by solving the equation

$$\sigma_{tav} = p \int_{r_1}^{r_2} \frac{\left[1 + \left(\frac{r_2}{r_1} \right)^2 \right] dr}{\left(\frac{r_2}{r_1} \right)^2 - 1},$$

resulting in

$$\sigma_{tav} = pr_1/(r_2 - r_1).$$

The value of S_{13} from this will be about 5-9% lower. In the case of the Inconel flow tube of the sodium pump, the difference in method yields a significant but smaller difference.

These factors increase the degree of conservatism in the design of the loop.

The conservatism of the Code-based design can be judged by comparison of the maximum operating pressures, given in Table I, with the static bursting pressure as calculated by the formula presented on p. 310 of Ref. 10:

$$P_{SB} = \frac{2\sigma_y}{\sqrt{3}} \ln \left[\frac{r_0}{r_i} \left(2 - \frac{\sigma_y}{\sigma_u} \right) \right],$$

where

$$\sigma_y = \text{yield stress at } 1000^\circ\text{F} = (3/2)(15,700) = 23,500 \text{ psi},$$

$$\sigma_u = \text{ultimate tensile strength} = 3(14,000) = 42,000 \text{ psi},$$

and r_0 and r_i are taken for the closure tube of Table I, the portion of the loop having the lowest operating pressure.

For the Mark-II integral loop closure tube,

$$P_{SB} = 2.285 \times 10^4 \text{ psi (1526 atm)},$$

which is $4\frac{1}{2}$ times the rated operating pressure of the loop.

For the operational Mark-II loop, it was recognized that consideration must be given to stresses resulting from thermal effects, such as dissimilar thermal properties of materials, or thermal gradients. Raising the loop body temperature to the design temperature will generate stresses due to the differential thermal expansion between the Type 316 stainless steel of the test section riser and the 26-in.-long ALIP flow tube of Inconel X-750 in the downcomer. Other stresses would be generated by the unequal

temperatures of the T316 stainless steel connecting lines between the loop-body weldment and the safety/dump tank (i.e., the fill, overflow, and blowout lines).

The differential thermal expansion between loop legs is analyzed in Appendix B. This analysis shows that the stress in the loop is within the allowable value obtained by extrapolating Code⁴ values to the design temperature of 1000°F. (Two versions of the basic loop, essentially the same but with somewhat different lower bends, were built: Mark-IIA and -IIB. Both are analyzed in Appendix B.)

Also covered in Appendix B is the analysis of the dump piping, comprising the blowout line from loop proper to safety tank, safety tank, and the fill and overflow lines from tank to loop proper. This analysis results in a conservative estimate of the system stresses, since the model used was two-dimensional, while the actual loop is three-dimensional and more flexible. The smaller, 5-ft-long overflow tube was neglected, because of its high flexibility. Throughout the analysis, the rectangular valve bodies and their weldable port projections were considered to be essentially rigid, because of their massive geometry. The replacement of the mechanical valves by a stainless steel fitting does not alter the analysis.

Two cases were considered for analysis. Case I corresponds to the steady-state pretransient operational condition of the Mark-II loop, with the blowout line maintained at 400°F, the mechanical valve and lower fill line at 125°F, and the burst disc intact. This distribution of temperature in the auxiliary loop is reasonable, because of the heavy thermal insulation covering the entire system, and of the thermal isolation of the mechanical valve, lower fill line, and safety tank from the hot loop by the liquid-cooled freeze plug.

Case II serves as a limiting calculation, with the blowout line at 900°F and the temperatures of the remainder of the auxiliary loop unchanged.

In both cases, the highest stresses occur at the segment of the auxiliary loop containing the mechanical valve in the fill line. For Case I, the maximum stress calculated was 9,407 psi, at the fill line valve, with a stress of 6,370 psi at the rear of the line nozzle to the loop, and a stress of 3,401 psi at the weldment of the fill line to the lower bend of the loop proper. None of these stresses are comparable to the yield strength of the stainless steel; hence, there would be no distortion in the system as a result of normal steady-state operation of the loop at temperature.

In Case II, the 900°F temperature of the blowout line corresponds to the limiting condition to be realized in the event that an overpressure ruptures the burst disc and discharges the molten sodium from the loop

proper into the safety tank. The resultant stresses calculated were: 33,317 psi at the fill-line valve, 21,563 psi at the burst-nozzle loop, and 11,510 psi at the fill-line/loop weldment.

These stresses realized in the auxiliary system are secondary stresses resulting from the thermal expansion of the blowout line during a thermal excursion, from 400°F to the temperature of the loop sodium. Since the valve releasing the sodium from the loop into the blowout line is a simple rupture disc, the excursion must be considered to be a single-time event; any analysis related to cyclic operation of the blowout line would be meaningless.

The Code,⁴ for cases not requiring analysis for cyclic operation, specifies that the limit of stress intensity for secondary stresses plus bending is to be defined as $3S_m$, where

$$S_m = \frac{(S_m \text{ at } 400^\circ\text{F}) + (S_m \text{ at } 900^\circ\text{F})}{2} = \frac{19,400 + 14,000}{2} = 16,700 \text{ psi.}$$

Accordingly,

$$3S_m = 50,100 \text{ psi.}$$

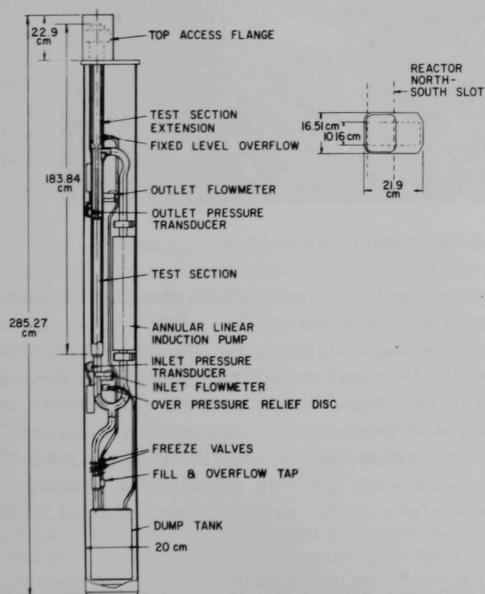


Fig. 3. Line-drawing Layout of the Mark-II Integral Sodium TREAT Loop. ANL Neg. No. 112-9204 Rev. 1.

Hence, the stress at the burst-nozzle loop ($\sigma_H = 21,563$ psi) is well below the limiting stresses allowed for thermal-expansion stresses and is far below the stress limit defined by the ASME Code.

III. DESIGN DESCRIPTION OF THE MARK-II LOOP

A. Loop

The Mark-II loop (see Fig. 3) is enclosed within a welded Type 304 stainless steel, double TREAT fuel can, with a wall thickness of 0.127 cm, a 20.32- by 10.16-cm cross section, and an overall length of 260.86 cm. The test-section extension of the loop passes through and is welded into a 21.9- by 16.51-cm top plate, which is bolted into and seals

the top of the enclosure can. A protective hood covers the top access flange of the loop and is hermetically sealed to the top plate, leaving the remaining half of the top plate available for through-connections to the exterior of the loop within the enclosure. A pair of multicontact, pressure-sealed electrical connectors furnish entry for instrument and electrical-power leads, and miniature quick-disconnect valve penetrations through the top plate furnish air and gas flow or pressure for component cooling or inert atmospheres. A valved, small-gauge pressure line supplies the inert gas pressurization to the supply-dump tank. The bottom of the enclosure is closed by a seal-welded plate, to which the indexing fuel can pins are bolted. Figure 4 shows the assembled loop structure, before outfitting.

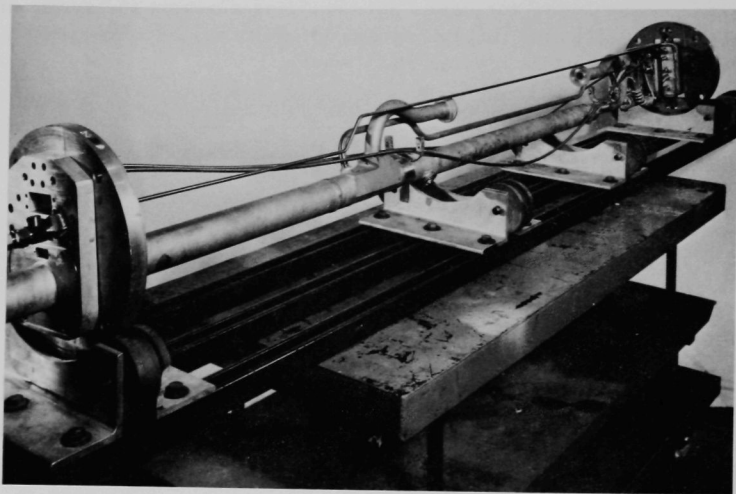


Fig. 4. Mark-II Loop Assembly before Outfitting. ANL Neg. No. 112-9514.

The test section is located in the loop leg opposite the sodium pump, with an extension above the loop proper, through the top plate of the enclosure can and into the plenum above the reactor core. Access to the loop interior for experimental loading and internal maintenance is made through a top closure flange, which consists of a heavy cap centrally penetrated by a fuel-thermocouple-exit assembly and sealed into place with a Conoseal clamp. Since this closure flange is outside the loop enclosure can, well away from the heat sources associated with the loop proper, the sealing clamp is fabricated of Type 316 stainless steel instead of the Inconel X-750 used elsewhere.

The fuel holder, with a removable extension, is loaded into the test section through the top access flange, and the closure of the flange by the tapered clamps exerts a predetermined downward axial force on the holder

through compression of a stack of Belleville washer springs. The force on the holder assembly presses the hemispherical base of the fuel holder into a 45° conical seat in the bottom of the test section, resulting in a line-contact seal between the holder flow channel and the flow tube of the loop body.

The test section has an ID of 3.254 cm, a wall thickness of 0.917 cm, and an overall length of 75 cm, which permits accommodation of fuel elements over 65 cm long. At the inlet and outlet of the test section, there is a 12.7-cm-long instrumentation section. The upper section is fitted for the measurement of flow and pressure. The lower section is fitted for the measurement of pressure. The flow measurement is made from the lower bend.

The total loop volume of sodium when filled to the design level is 1313 cm.³ For loops containing the mechanical valves, the loop is filled by pressurization from a supply tank located in the bottom of the double dummy TREAT fuel can and connected to the bottom of the loop through a high-pressure, bellows-sealed valve and a sodium freeze plug. A fixed level of sodium at temperature is maintained by an overflow line, which is controlled by a mechanical valve* and a freeze plug. The mechanical valves* are remotely actuated by flexible-shaft driver gears, and the freeze plugs are closed by coolant circulating through copper tubing thermally bonded to sections in the piping above each mechanical valve.

The supply tank is pressurized with an inert gas, which also furnishes an inert gas blanket above the sodium in the loop. When the loop has been filled and is in operation, the supply tank serves as an auxiliary safety tank, with overpressures vented into its volume by a calibrated rupture disc located above the sodium level in the test-section extension. The rupture disc is rated at 340 atm at 25°C to match the loop design rating.

The heat required for steady-state operation of the loop is supplied electrically and is divided into two independently controlled, physically separated heater circuits. Loop heaters consist of thin metal-clad high-capacity 230 V ac, clamp-on electric heaters fastened around the long, straight test section and high-capacity flexible heating tapes rated at 870°C, wrapped closely about the remainder of the loop between the test section and the sodium pump, where application of rigid heaters is impractical. The sodium pump is not externally heated; indeed, the inherent electrical losses associated with the operation of the pump pose a problem of cooling rather than heating.

*Mechanical valves of proper size having the same pressure rating as the loop are not commercially available. Thus, the valves are protected by the freeze plugs. Although this arrangement was verified by successful prooftesting in the loop, it was decided that the mechanical valves represented a potential weak spot in the design. After a review of operational experience with the first four Mark-II loops, these valves were replaced by steel sections which isolated the freeze plugs from the safety tank. Swagelok fittings in the sections permit filling and draining operations.

The second, or auxiliary, heater circuit is applied to the multi-purpose tank below the loop proper, and the dump/fill and overflow lines and valves. The supply tank is heated by braid-wrapped, asbestos-insulated Nichrome heater wire, held in place against the tank outer wall by lightly spot-welded ribbons of stainless steel foil. Fill and overflow lines and valves are wrapped with the high-temperature, flexible heating tapes. The entire loop, with the exception of the sodium pump, the mechanical valves, and the pressure-transducer assemblies, is coated with a porous, silicate-based thermal insulation, which is applied as a moldable wet felt over the loop and auxiliary heaters. During pre-transient operation of the loop and while the loop sodium is maintained at the desired initial temperature, the auxiliary heaters are not energized, and the auxiliary portions of the facility are thermally isolated from the loop body by the chilled freeze plugs. Figure 5 shows a fully assembled, outfitted Mark-II loop next to its containment can.

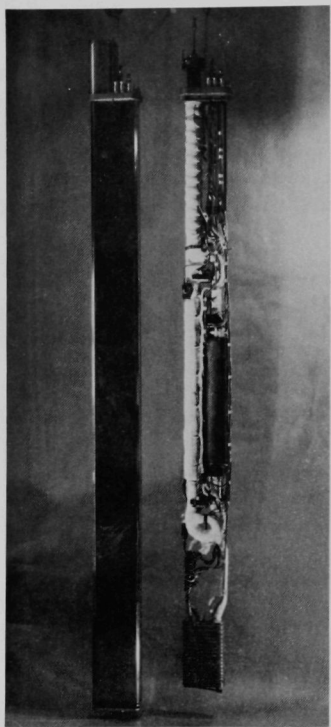


Fig. 5. Finished Mark-IIA Loop next to Loop Containment Can. ANL Neg. No. 900-727.

The Mark-II loop is fully instrumented for the measurement of sodium flow, temperature, and pressure under steady-state and experimental transient conditions. The operating temperatures of loop components are continuously monitored with shutdown interlock protection for the facility in the event of excessive temperatures.

Sodium flow is measured at the inlet and outlet of the test section by means of electromagnetic flowmeters. The thick walls of the loop made the use of the conventional permanent-magnet flowmeter impossible in the limited space available within the loop enclosure, since a magnet of sufficient strength to establish the required field in the liquid metal would be several times too large. Hence, dc electromagnets are used with high-curie-point Armco iron armatures wound with ceramic-insulated copper wire and supplied with a constant direct current. The constant-current dc power supplies have a current range of 0.5 to 7 A, a maximum voltage of 100 V, and a 0.01% line-and-load regulation capability. Each flowmeter is calibrated over a wide range of field intensities and temperatures. During loop operation, the temperature of each magnet is continuously monitored.

Sodium pressure is measured at the inlet and outlet of the test section by pressure-transducer assemblies of the standoff type developed for sodium-filled systems and used on the Mark-I integral loop.^{4,5}

B. Loop Instrumentation and Control

Specialized instrumentation is required for control of the loop operation and for the recording of data, under both steady-state and transient conditions. The instrumentation and control system was designed around existing components and techniques; it has a minimum of complexity and provides for automatic safety measures. Systems external to the loop include an instrument indication and control console, an ALIP power module, a silicone-oil circulation/cooling unit, and the loop-systems electrical-power chassis.

Instrumentation and control of the Mark-II integral loop have two modes: (1) the attainment and maintenance of a predetermined steady-state system condition prior to a programmed TREAT power transient, and (2) the accurate and precise measurement of transient data during and following the reactor excursion.

Temperature, pressure, flow, electrical power, and valve conditions are measured. All parameters are sensed by detector units of conventional design, with remote measurement, indication, and control.

Spiral-armored, asbestos-insulated, Chromel-Alumel thermocouples are used for the measurement of temperatures of the loop system and its sodium. The temperatures of sodium, loop-system components, and heat-sensitive sensors are continuously monitored. The thermoelectric signals from a loop monitor point drives high-impedance electronic controllers, which provide fixed-point control of loop temperature. Heat inputs, and hence temperatures, are controlled by ON/OFF switching of electrical heater power, supplied through adjustable autotransformers.

Most of the thermocouple outputs are monitored by remote indication only, with manual adjustment of heater-circuit controls made as required. Monitor thermocouples are located on the laminated yokes and coils, within the cooling housing of the sodium pump, in an internal well within the sodium safety tank, in small wells just ahead of the pressure-transducer diaphragms, and on each of the flowmeter dc-magnet armatures. Thermocouples are located on each of the freeze-plug valves placed in the overflow and fill lines between the loop proper and the storage tank. These sensors monitor the temperature of the silicone-cooled freeze-plugs and the thermocouple signal interlocked to the reactor controls; transient initiation is prohibited if the freeze-plug temperature is above a preset value. An additional interlock is actuated by a monitor thermocouple located on the safety-burst-disc blowout line to prevent a reactor transient unless the line temperature is well above the melting point of sodium.

The loop sodium flow is measured by dc-magnet electromagnetic flowmeters at the inlet and outlet of the loop test section. Output of the electromagnetic flowmeters is preamplified by low-gain, wide-band dc amplifiers and is continuously monitored on remote indicator-recorders.

Loop sodium pressures are measured by pressure transducers at the test-section inlet and outlet, as indicated in the preceding section.

Auxiliary instrumentation is provided for the indication and control of pretransient system parameters and component condition. Input electrical power to the ALIP and to the heater circuits is indicated by meter. Control of the autotransformer ALIP power supply is provided at the loop control console.

The desired operating temperatures of the ALIP and the freeze valves are obtained by independent adjustment of throttle valves placed in the inlet lines of recirculation loops supplying a cooled, low-viscosity silicone fluid. A flow-switch in the silicone-coolant supply is provided as additional protection against pretransient system fault. The switch is interlocked with the reactor-transient controls and is in series with the safety interlocks from the freeze valve and blowout-line temperatures.

An inert gas blanket is maintained within the sealed stainless steel secondary containment can. Gas flow is metered for valve adjustment for purge and maintaining the blanket. Exhaust is through the TREAT reactor stack.

IV. QUALITY STANDARDS, CONTROL, AND ASSURANCE

A. Quality Levels

For a single, complete integral loop, several levels of quality requirements can be defined, depending upon the usage of the loop in meltdown experiments. Since the Mark-II loop comprises three interfaced, interconnected systems, which are potentially subject to widely varied stresses during loop operation, the quality required ranges from the highest possible to the simple functional.

The loop body is required to contain sodium and fast-reactor fuel (including plutonium and/or fission products) safely at the design rating of internal pressure and temperature. The loop body also is considered to include a portion of the interconnecting lines between the circulating (primary) portion of the loop and components of the auxiliary system, specifically the overflow line and the fill-line loop attachments, from the loop to the sodium freeze plugs.

The auxiliary system is required to contain sodium (liquid and/or vapor) and fast reactor fuel following a single-time, abnormal operation of the loop, during which the contents of the loop are vented as a result of internal overpressure. The system includes the multipurpose dump/safety tank, the connection lines between valves and tank, and the gas-pressure supply line. The auxiliary system will operate at a considerably lower pressure-temperature rating than the primary loop body.

The secondary system, which encloses the total loop assembly, is a secondary containment volume, which serves as a low-pressure and low-temperature container for sodium spills. It encloses gas- and liquid-coolant lines, and the electrical-power and instrumentation leads. Although the secondary system does not require high-strength, high-temperature capability, its integrity must be reliable within the less stringent demands for preventing leakage of sodium and possibly fine active particles.

Accessories used in the three systems noted above are those components that provide the means for attaining and controlling pretransient loop operating conditions, and for indicating or recording operational and experimental data. Pressure transducers, in NaK-filled standoff assemblies, penetrate the loop body and are attached at penetrating pressure taps by means of O-ring-sealed flanged joints; experimental thermocouples are located within the loop test section and require a sealed penetration of the primary containment. These accessory devices must not compromise the primary containment.

Flow and temperature sensors required for loop operation are external to the loop, as are the electrical heaters, and require no penetration of the primary containment. The leads to external sensors and powered devices and to the gas- or liquid-coolant lines are external to the loop and within the secondary containment, with sealed penetrations through the top closure of the secondary housing. Components which are outside the loop and within the secondary containment require only a high order of functional reliability, since their failure affects the operation of the loop without compromising its integrity.

The rationale for the extreme rigor of quality of the primary containment was founded on the intrinsic uncertainty in the probable values of the experimental parameters of greatest interest in the meltdown of reactor fuels in the presence of liquid-metal coolant, and includes the following:

1. Amplitude or pressure pulses generated by the failure of fuel and resultant reaction.
2. Rise time of the generated pressure pulses.

3. Rate of fuel-to-coolant-to-loop heat transfer.
4. Efficiency of thermal-energy conversion to work done against the loop containment.

The use of the Mark-II loop for experiments examining the possible occurrences of these four accident phenomena prompted the selection of the following general quality criteria:

1. All peripheral points of the primary normal-operation pressure containment must have the highest structural integrity. This includes the loop body, fill line, freeze plug, overflow line, freeze-plug burst line, and pressure-sensor assemblies, as well as the ALIP.

2. Components of the auxiliary system that function as pressure containment under abnormal conditions must have essentially the same structural integrity as the primary containment, although at somewhat lower temperature-pressure levels established by accident analysis. These include the multipurpose storage-safety tank, the mechanical shutoff valves, and the helium-gas line to the tank.

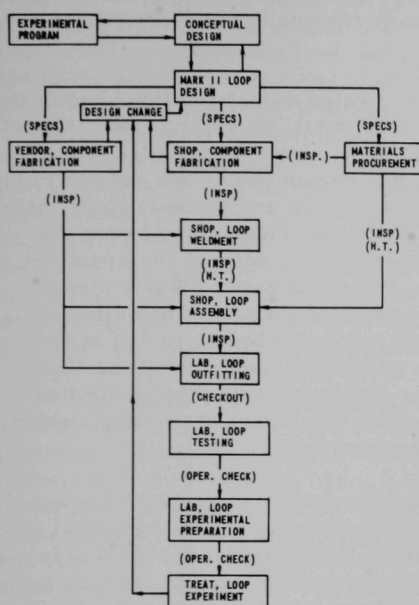
3. The secondary containment should have sufficient integrity to contain the consequences of a loop leak safely. This containment consists of the double TREAT-element stainless steel thin-walled enclosure can for the loop, which is hermetically sealed at the loop top plate, and of the cover, which is sealed to the top of the top plate in order to enclose the top access flange.

4. The system of external accessory components must have sufficient integrity to contain the flow of blanket and coolant gas and coolant liquids without failure during normal operation of the loop, or to suffer abrupt direct contact with high-temperature sodium and/or fuel (in the event of an accidental loop breaching) without danger. The accessories within the secondary containment are operationally necessary, but are not involved in the direct containment of the loop experiments. These include the gas and silicone-oil cooling lines and connectors, electrical leads, and external structural supports. Their reliability and ability to withstand "operational accidents" without damaging the loop must be demonstrated.

B. Quality Control and Assurance

The quality criteria and control followed in the construction of the integral loops, with regards to standards for materials, fabrication techniques, inspection, and evaluation control, were established by the Engineering Physicist in charge of the loop development. The sequence of development and construction may be outlined briefly as follows:

1. Select most applicable design codes and standards.
2. Determine the necessary levels of conservatism required.



(SPECS) - DESIGN SPECIFICATIONS
(INSP) - INSPECTION
(H.T.) - HEAT TREATMENT

Fig. 6. Flow Diagram of Mark-II Loop Development

3. Take only those exceptions to the selected Code which are absolutely required.
4. Establish the design before starting fabrication.
5. Minimize design changes during fabrication.
6. Maintain day-to-day surveillance to ensure adherence to specifications.
7. Record, in most convenient fashion, all pertinent specification, procedural and historical data for each unit.
8. Proof-test each unit on completion and before experimental use. (See Appendix A for the proof-test form.)

The above may be seen implicitly in Fig. 6, which is a simplified flow diagram of the work on the Mark-II loops through the experimental use in TREAT. The documentation is diagrammed in Fig. 7.

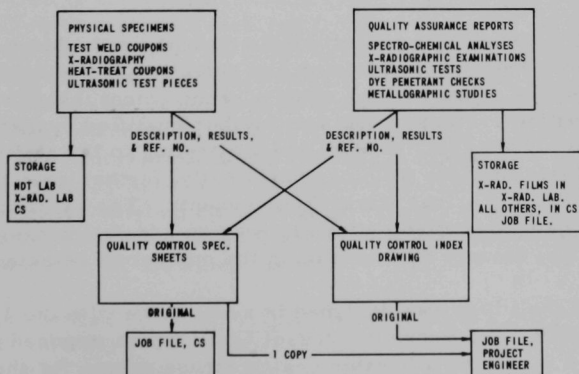


Fig. 7. Diagram of Loop Documentation

The exceptions taken to the ASME Code further to assure the quality in the Mark-II loop involved acceptance standards of materials and welds, permissible operations on the loop during fabrication, the qualification of welders, and specification of minimal temperatures for heat treatment of the loop weldments.

Although the colloquial expression "water clear" is often used in the weld shop in reference to the quality of weld joints, no explicit definition of the term's meaning is given in the ASME Code. Instead, the acceptance standards prescribed in the ASME and other design Codes are related to the acceptable type, sizes, and distributions of surface and internal flaws, usually designated as porosities. Because of the demanding service for the Mark-II loop, the term "water clear" was explicitly defined and specified to apply to stock materials, components, and weldments. "Water clear" was defined as that condition in which no detectable flaws of any kind are revealed in the material, component, weld, or assembly examined at the maximum sensitivity established for the particular method of inspection, i.e., whether radiographic, ultrasonic, or dye-penetrant. This definition is descriptive of a perfect part of weld within the limits of existing standards. No exception to this criterion was permitted.

In the event of a flaw in a weld, a procedure for repairing the weld was established which explicitly rejected the Code-permitted "removal of the flaw by grinding" followed by rewelding. A flaw within the zone of fusion in a weld was specified to be removed only by cutting (i.e., by turning, milling, etc.) without grinding. This more rigorous requirement on the repair of weld faults was specified to prevent the imbedment of abrasive particles in the relatively soft stainless steel weld metal and to minimize the degree of work hardening of the weld at the critical plane of fusion during the remelting process of repair. No repair of stock materials (bar or pipe) was permitted.

The requirement for perfect welds throughout the Mark-II loop necessitated more rigorous examination and selection of the welders who were to make such welds. Thus, it was made a requirement that the welder must be a Code-certified craftsman who was further qualified by test on the Mark-II loop weldments. This specification, while attesting to the ability of the welder to perform flawless welding consistently, further gave him prior experience in welding actual Mark-II components. The extra qualification of the welder, using certified materials, was an added expense, but it resulted in eventual savings by minimizing the number of rejected welds.

The Mark-II loop was designed in accordance with the 1965 edition of the ASME Boiler and Pressure Vessel Code, which imposed a conditional requirement on the listed allowable design stress values for the T316 stainless steel, namely, heat treatment of the metal to a minimum temperature of 1800°F. Although it is widely accepted that austenitic stainless steels

have zero notch sensitivity, and although precipitated carbides do not have a detrimental effect on the macroscopic physical properties of such materials, we were aware, out of past experience, of anomalous weld failure in relatively thick-walled welded structures fabricated of austenitic stainless steel when subjected to shock loads. Subsequent examination of such failures led to the realization that the high-heat, restricted-zone welding of relatively thick-walled components of austenitic steels can result in large differentials of carbon diffusion into and across weld zones, and the precipitation of continuous, subgranular planes of carbides and ferritic structures, which may present, under shock loading by distributed stresses such as those from a high internal pressure pulse, the appearance of high notch sensitivity. The acute awareness of the designer that the Mark-II loop consisted of exactly such a welded structure, fabricated of relatively thick-walled components and diverse history, and possibly to be subjected to shock loading by pressure prompted the adoption of a heat-treatment requirement more rigorous than that stipulated by the base Code.

The Code requirement of a minimum heat-treatment temperature of 1800°F was increased to 1900°F (1900 + 50°F), with a water quench, for all portions of the loop primary containment comprised of heavy-walled components joined by welding. This directed such heat treatment particularly to the loop-body weldment and the multipurpose tank. All other components of the primary containment system (including the auxiliary connecting lines, and excepting the mechanical valves and helium line) were to receive the same heat treatment, but before their assembly by welding.

As a means of obtaining assurance as to the chemical content of the material from which a particular component was to be made, it was found necessary to check certifications for particular elements from independent testing laboratories, with retests or comparisons with secondary standards required in cases of discrepancy. Such check analysis was required for every piece of stock material received from a vendor. A general procedure was established that required material certification before any fabrication process was begun. The chemical analysis was made for chromium, nickel, molybdenum, and carbon in the case of the T316 stainless steel, and a complete analysis was made of all Inconel X-750 material. Weld filler wire, purchased only in spools, required a chemical analysis of a single sample if the spool weighed $2\frac{1}{2}$ lb or less, and of three samples, from head, middle, and tail, if the spool weighed 25 lb. Fusion rings, cut from sheet material, were checked for chemical composition by analysis made of samples taken from edge and center of the stock sheet.

Design changes from the original were held to a minimum.* The burst disc was initially located above the free surface of sodium, porting the closure tube to vent the inert gas above the loop sodium; this was similar

*The original design is documented in Ref. 11.

to the burst-disc overpressure relief provided in the Mark-I integral loop. Later, the port was relocated to the riser side of the loop lower bend, below the inlet-instrumentation section. This change removes the safety line from the crowded region around the pump and test section. In addition, with the lower position, disc rupture will relieve the pressure within the loop and simultaneously remove the sodium from the source of heat. (Safety implications of continuing contact between hot fuel and sodium were emphasized during the loop development.)

Pneumatic two-way piston actuators for the mechanical valves were replaced with flexible rotary drive cables. The valves were eventually removed, as described earlier.

The thermocouple well below the test section, intended to provide control signals for the sodium inlet temperature, was eliminated, because of difficulty in controlling welds in this extreme geometry. Sodium temperature is monitored by means of a thermocouple inserted through the closure cap of the loop, along with experimental fuel thermocouples.

The rectangular dump tank was redesigned after a test indicated that the original design was inadequate. The internal stiffeners were augmented by the addition of cross tendons between the flat sides of the tank; the tank currently used holds 4000 psig internal pressure.

During the fabrication of the Mark-II loops, a day-to-day surveillance and supervision of operations and inspections was maintained to ensure the necessary control of quality. Depending on the status of work on various aspects of the construction, the time was spent in examination of weld radiographs, ultrasonic records, spectrochemical reports on materials, metallographic studies of sample welds, components received from vendors, and consultation on fabrication procedures. The necessity for continual supervision was due in part to the demonstrated need to confirm vendor certifications of chemical compositions, heat treatments, and mechanical histories. No exception to or deviation from the given specifications was permitted. When design change, level of difficulty, or degree of adequacy indicated that a particular specification had to be changed, the change was made only after quality equivalence or quality improvement was assured.

Quality equivalence was based on the basic stipulations of the design code in choosing options or alternates as prescribed. Design specifications required full penetration welds and full radiographic postweld examination, both in the loop-body weldment and in the loop assembly. By sequentially welding the various components together, with cleanup and radiographic inspection performed on each weld before making the next, the weld specifications were applied without difficulty in the loop-body weldment. Full penetration of weld joints in the loop assembly was determined by full radiographic examination, with the exception of the reinforced safety tank.

The closed geometry of the roughly rectangular tank made the postweld radiography of the 16 transverse plug-welded tendons impossible; full penetration was ensured by welder qualification with weld samples in which an excess of weld metal was obtained in the internal tendon-wall fusion area. This exception was allowed because of the lower pressure-containment requirement of the loop auxiliary piping system and because the safety tank is pressure-tested during the loop proof test.

To provide a convenient record for the sequence of fabrication processes, a pictorial method of providing an annotated index of quality assurance was adopted. The index for each loop consisted of a copy of the serialized drawing of the main loop weldment and a copy of the drawing of the loop assembly, on which the quality-control data for each component and related processes were detailed. Data shown for each component included:

1. Material chemistry certification, referred to the Central Shops requisition number under which there is listed a chemical report.
2. X-radiographic examination, by date and signatory initials of the specialist accepting the material.
3. Ultrasonic examination, by date and signatory initials of the specialist accepting the material.

Data shown for each weld included:

1. Certification of the weld filler wire, referred to the Central Shops requisition number, under which there is listed a chemical report.
2. Name of the qualified welder.
3. X-radiographic examination, by date and signatory initials of the specialist accepting the weld.
4. Any conditional comments pertaining to the particular weld.

The two quality-control index drawings for each individual Mark-II loop, referenced copies of the material and heat-treat reports, a copy of the proof test report, and a complete set of engineering drawings comprised a comprehensive record of quality assurance for each loop. The context of the index drawings is indicated in Fig. 7, which illustrates the distribution of quality-assurance data and documentation.

At present, the formal quality-control specification sheets established under the ANL quality-assurance program provide the main documentation for each loop. However, the quality-control index drawings for each loop were sufficiently useful during the period of development that

they were retained in the new documentation process set as part of the ANL quality-assurance program, through completion of the first three Mark-II loops.

Early in the construction of the Mark-II loops, it became obvious that a major problem was involved in the procurement of the heavy-walled seamless tubing required for the primary containment, in the SA-312 Type 316 stainless steel specified, and with the necessary chemical composition and nonstandard sizes. The minimum order (10,000-ft mill-run in many cases) required by possible suppliers made direct purchase of the tubing prohibitive in cost and very long; indefinite lead times left no assurance as to when construction could begin. As a result, the only solution found was the fabrication of every tubular component of the loop proper (the loop "body") from selected bar stock, equivalent in properties to the specified SA-312, T316 stainless steel. This entailed gun drilling and boring the tubular parts from carefully certified bar, forming the tubes into the small-radius bends where required, and sequentially joining the components to make the loop body.

Since the completed components were to meet the requirements for Group A Finished Tubular Products, the bar stock was required to meet criteria more severe than the Code requirements for bar materials. X-radiography and ultrasonic nondestructive test methods were specified as the inspection techniques to be used throughout the selection of material and the fabrication processes, since these are the only Code-prescribed methods which are applicable to the Mark-II loop. Bar selected from available stocks, of proper size and nominally correct chemical composition, was first examined by pulsed ultrasonics to eliminate those specimens with unacceptable internal flaws. The reference defects prescribed by the Code for the ultrasonic examination of bars (Section III, Art. N-322) are a $1/2$ - x 3-in. hole in a $2\frac{1}{2}$ - x 30-in. bar for the longitudinal wave technique, and a 1- x 0.075-in. groove in the same bar for the shear-wave technique. These were considered far too large in size to be meaningful in this case.

With the object of ultimately obtaining a Group A Finished Tubular Product from the bar stock, the ultrasonic reference defect was decreased in size to $1/32$ -in. diameter x $1/2$ -in. depth for the initial selection of the bar. Following gun drilling of the round bar, the finished straight sections of tubing were examined by ultrasonic and radiographic methods, as prescribed by the ASME Code, all pieces indicating perceptible flaws being rejected. After a mechanical forming process, as required, the finished product was again radiographically examined for conformance with the Code requirements for Group A Finished Tubular Products.

Inspections of finished weld joints were performed as far as possible according to the ASME Code, with the exception of the establishment of criteria for acceptance or rejection. The exception taken from the Code in the

case of tungsten inert-gas welds (TIG) consisted of the specification that all completed welds were to be totally clear of flaws detected by full radiographic examination, rather than to conform with the Code, which allows detectable flaws below acceptable flaw-size limits. Although the Code prescribes that finished welds be inspected by at least two of the several methods given, as applicable, and despite the desirability of using the ultrasonic and radiographic techniques throughout the system, the small scale and complexity of the loop system rendered the use of the ultrasonic method in the inspection of finished welds impractical. As a result, the welds were checked initially by the Zyglo dye-penetrant method to indicate gross subsurface and superficial surface flaws, and then they were fully X-radiographed. In addition, all welds were reexamined after heat treatment by the dye-penetrant method.

In certain cases (such as in the final weld of the Inconel pump flow tube) the alternative method of electron-beam welding was required as a means of precisely controlling shrinking and to eliminate the necessity for adding extra metal during the welding process. It was recognized that no standards existed by which the weld could be inspected by either the ultrasonic or radiographic method, because of the extremely small size of the electron-beam weld zone. Since all welds were specified to be full penetration and completely clear, it became necessary to establish some method by which the criteria for acceptance might be met. During the welding process a massive internal backup ring of Inconel was used, with a minimum of 40% penetration of the electron beam into the ring specified. After welding and dye-penetrant examination on both the inside and outside surfaces of the tube, the penetration was determined by machining the ring out of the inner bore prior to full radiographic examination. While wholly empirical in method, this technique ensured full penetration in welding, whereas neither radiography nor ultrasonic inspection was capable of detecting incomplete penetration.

V. PROTOTYPE LOOP TESTING

Extensive testing of the prototype loop was performed before the actual proof test at high pressure. This testing afforded an opportunity to check the actual operation of the device and its ability to withstand operational incidents.

The prototype was the first of the Mark-II integral sodium loops and contained certain deviations from the loop specifications that were considered acceptable in a loop to be used for preliminary tests and development of operational techniques. These deviations consisted of deficiencies that would be most likely to occur during fabrication and result in some compromise of the specifications; detailed testing of the prototype thus could confirm the design and specifications with a measure of conservatism.

Deviations included one weld with an inclusion consisting of extraneous electrode metal,* internal undercutting of two welds from incomplete penetration,* two welds with filler material of unverified chemistry, and alignment of loop-pump flanges that was outside the specification for degree of parallelism. Despite the deviations from the stringent specifications demanded for the Mark-II loops, it was recognized from the outset that the final judgment as to the quality and/or usability of any given loop would rest upon the outcome of the final proof test of the particular unit at pressure and temperature. Hence, successful proof test of the prototype would qualify the loop for experimental use in the meltdown program while in no way justifying the relaxation of the quality-control specifications previously enumerated as a means of ensuring a conservative design.

Specific points of potential concern which were covered during the prototype testing included:

1. Consequences of electrical malfunction or failure in the ALIP.
2. Consequences of silicone-oil leak inside the secondary containment.
3. Consequences of possible thermal differential between the two loop legs.
4. Consequences of a sodium leak.
5. Prototype proof test at high temperature and pressure with flowing sodium.

The results are summarized below.

Consequences of Electrical Malfunction or Failure in the ALIP.

Extensive bench tests with the prototype ALIP had demonstrated that the pump tube would survive internal electrical breakdown and shorting of one phase to ground. Although this electrical fault did reduce the efficiency of the pump, its containment integrity was not affected, and it was used with the prototype loop. During the approach to operating temperature during the first full prototype loop test, the ALIP was operated at about half-maximum current to supplement the heat input by the external resistance heaters. After the loop had reached 425°C, the flow of ALIP silicone coolant was reduced to near zero. Relatively high temperatures in the ALIP and its coolant circuit resulted.** The ALIP stator temperature reached about 550°C, well above the temperature limits of the epoxy potting compound used for the ALIP coils. Extensive charring of the epoxy was found upon inspection. In addition, the ceramic insulator of one of the connectors

*Deviation from loop specifications only, acceptable within the Code.^{3,4}

**The early ALIP coils were wound with copper wire and encapsulated with epoxy. The present loops use acrylic-coated, anodized aluminum ribbon. The following refers to the epoxy-encapsulated coils.

carrying power through the pump shell broke. Charred epoxy was flushed out, the insulator was repaired with epoxy, and the prototype ALIP was returned to service.

Consequences of Silicone-oil Leak inside the Secondary Containment. Questions had been raised concerning the use of the temperature-resistant silicone oil as the coolant for the ALIP and the consequences of a coolant spill putting silicone oil in direct contact with the loop while at operating temperature. The Dow-200 low-viscosity silicone fluid was selected for its excellent temperature stability, but it was recognized that the liquid would burn under the proper conditions of temperature and in the presence of oxygen. During this first prototype test, the break in the through-connector caused approximately 2 liters of the silicone to spray out into the can, flow down over the lower half of the loop, and collect in the bottom of the container. Although the silicone saturated the insulation and heaters of the hottest portion of the loop, the only result was the appearance of a large quantity of smoke; there was no ignition of the silicone, nor damage to insulation, heaters, or any component of the loop.

Consequences of Possible Thermal Differential between the Two Loop Legs. The problem of steady-state design arising from the different thermal-expansion coefficients of T316 stainless steel and the Inconel pump tube has been mentioned in Section III (see Appendix A). However, concern existed that, during use of the loop for meltdown experiments, the heat generated in the fuel sample could overheat the test-section leg and damage the loop by differential thermal expansion. In the next test, the ALIP Inconel tube temperature was set at 66°C (this temperature is below the sodium melting point; solid sodium in the loop circuit prevents sodium circulation and thus serves to aid in establishing a temperature differential between legs). The temperature of the test-section leg was raised to approximately 400°C. Following this 334°C differential test, the ALIP unit was removed from the loop for examination of the flanges and O-rings. While the pump was out of the loop, the pump interflange distance was found to be unchanged (within a possible limit of 0.005 cm) despite the high temperature differential between the Type 316 stainless steel test-section side and the ALIP flow tube of Inconel X-750. This provides an indication that the compound-curved offset bends of the loop, above and below the ALIP, react to the expected axial load of differential thermal expansion as massive, but efficient, springs. A small flange leak opened up, however* (see below).

*The seal leak at the pump flange was the result of using a design in which flange clamps were deliberately slightly sprung open, to protect the contact side of the flange. With this type of clamp, the O-ring-seal capacity was discovered to be a function of the clamp spring constant as the bolts were tightened; the seal leaked at about 4200 psi, whether the fluid was inert gas or water at room temperature, or was sodium at about 200°C. Replacement of the sprung clamps with straight clamps provided a seal at half the previous bolt torque, which was tested up to 10,000 psig in tests outside the loop and functioned satisfactorily in loop proof tests.

Consequences of a Sodium Leak. During the 334°C differential test, the lower O-ring seal of the ALIP developed a small leak,* and about 500 cc of sodium estimated to be at a temperature of approximately 300°C ran down onto the lower regions of the loop. In the process, the sodium contacted silicone-impregnated thermal insulation. The sodium froze safely in the bottom of the secondary containment can.

Prototype Proof test at High Temperature and Pressure with Flowing Sodium. The proof test of the prototype loop was the final test conducted on the prototype loop and pump to demonstrate design adequacy. The loop was run at 427°C** and 6300 psi. Maximum ALIP shell temperature was 77°C, indicating quite adequate cooling.

*Op. cit., see previous page.

**Down from the 538°C of subsequent loops because of limitations on the prototype heaters.

APPENDIX A

Proof test Form for the Mark-II Integral LoopPROOF PRESSURE TEST REPORT, Mark-II Integral Sodium TREAT Loop

1 of 2

Loop No.: _____ Date _____

Loop Rating: _____ psig, at _____ °F (_____ atms, at _____ °C)

Type of Test _____ Location _____ Facility _____

Instrumentation:

Temperature: Sensor _____ Readout _____ Calibration _____

Pressure: Gauge _____ Range _____ Precision _____ Calibration _____

Flow: Sensor _____ Range _____ Precision _____ Calibration _____

Loop Volumes:

Sodium _____ Gas _____ of _____ Other _____

Temperatures:	<u>Start</u>	<u>Before Flow</u>	<u>After Flow</u>	<u>Test</u>
Loop Sodium	_____	_____	_____	_____
Test Section	_____	_____	_____	_____
Upper Bend	_____	_____	_____	_____
Lower Bend	_____	_____	_____	_____
ALIP Tube	_____	_____	_____	_____
Closure Tube	_____	_____	_____	_____
ALIP Shell	_____	_____	_____	_____
Fill Freeze	_____	_____	_____	_____
Overflow Freeze	_____	_____	_____	_____
Dump Tank	_____	_____	_____	_____
Silicone Feed	_____	_____	_____	_____
Silicone Exhaust	_____	_____	_____	_____

Flow:

Loop Sodium	_____	_____	_____	_____
Silicone Coolant	_____	_____	_____	_____
Air Coolant	_____	_____	_____	_____
Blanket Gas	_____	_____	_____	_____

Electrical Settings:

Flowmeter	Volts:	_____	_____	_____	_____
	Amps:	_____	_____	_____	_____
ALIP	Volts:	_____	_____	_____	_____
	Amps:	_____	_____	_____	_____

Main Heater, Amps: _____

Bend Heater, Amps: _____

Closure Heater, Amps: _____

Notes: _____

PROOF PRESSURE TEST REPORTRated Temperature; $T_r =$ _____ Rated Pressure; $P_r =$ _____Test Temperature; $T_t =$ _____ Test Pressure; $P_t =$ _____ *Proof Pressure Test Sequence:

<u>Loop Pressure Required</u>	<u>Dump Tank Press.</u>	<u>Loop Press. Rdg.</u>	PM	PM	<u>Δt, min **</u>
			<u>Time, Start</u>	<u>Time, End</u>	
Start _____	_____	_____	_____	_____	_____
0.5 P_t _____	_____	_____	_____	_____	_____
0.6 P_t _____	_____	_____	_____	_____	_____
0.7 P_t _____	_____	_____	_____	_____	_____
0.8 P_t _____	_____	_____	_____	_____	_____
0.9 P_t _____	_____	_____	_____	_____	_____
1.0 P_t _____	_____	_____	_____	_____	_____
† _____	_____	_____	_____	_____	_____
0.2 P_r _____	_____	_____	_____	_____	_____
(cooldown)					

REMARKS:NOTES:NOTES:

$$* \text{Test pressure, } P_t = 1.25P_r \left[\frac{S_{mt}}{1.4 \times 10^4} \right]$$

where S_{mt} = maximum allowable design stress at the test temperature, from Table PG-23.1, p. 145, for $T_t > 800^\circ\text{F}$, and from Table N-421, p. 37, for $T_t < 800^\circ\text{F}$, ASME B&PV Code, 1968.

**Time at the incremental pressure, 5-10 min.

†Loop pressure at 0.75 P_t or P_r , whichever is greater.

APPENDIX B

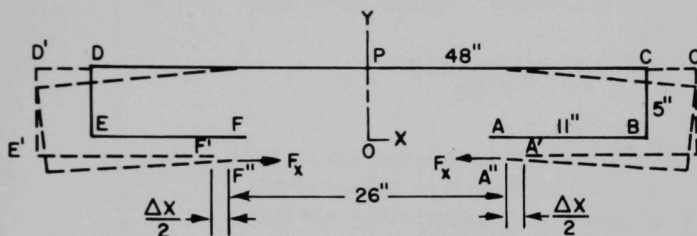
Detailed Stress Analysis for the Mark-II Loop

by

Israel Pollack and Arthur A. Frigo

Design and Engineering
Services Division1. Main Loop Weldment for TREAT Mark IIB

As a first approximation, we shall use the model shown in the following sketch to determine stress.



We assume symmetry about the Y axis. If we assume the Inconel section between A and F is not present, the open loop ACDF would expand symmetrically about the Y axis when subjected to a temperature rise. We could then assume either point O or point P as fixed. If we assume point P as fixed, the loop assumes a new position A'C'D'F'. If we assume the rigidity of the loop is much greater than that of the Inconel tube, we can replace Inconel with a flexible cable member that will now draw ends A' and F' together by an amount equal to the differential expansion between the stainless steel and the Inconel. Since the cable is flexible, no moments will be generated at A and F.

We shall follow the procedure in Mark's Mechanical Engineers Handbook, T. Baumeister, Ed., 6th Edition (1964), Section 5, "Pipeline Flexure Stresses Caused by Expansion or Movement of Supports," p. 88. Because we assume ends hinged, the end moment M_O at the origin vanishes. Because of symmetry $F_y = 0$. The equation for the end reaction at the origin in the X direction, F_x (Section 5, p. 89) is

$$F_x = \frac{EI\Delta X}{G},$$

where E is the modulus of elasticity at the working temperature, I is the moment of inertia of the cross section about the centerline, and G is a constant. We shall calculate G following the outlined procedure:

Section	s, in.	F, lb	G, in. ³
AB	11	0	0
EF	11	0	0
CD	48	240	1200
BC	5	12.5	42
DE	5	12.5	42
Total		265	1284

Assume the following values for the coefficients of thermal expansion:

$$\alpha_1 = 8.1 \times 10^{-6}/^{\circ}\text{F for Inconel};$$

$$\alpha_2 = 10.29 \times 10^{-6}/^{\circ}\text{F for stainless steel}.$$

Then

$$\Delta X = \delta_2 - \delta_1 = L(\alpha_2 - \alpha_1) \Delta T.$$

If

$$L = 25.875 \text{ in.}$$

and

$$\Delta T = 1000 - 70 = 930^{\circ}\text{F},$$

then

$$\Delta X = 0.0527 \text{ in.}$$

Assuming uniform I throughout the loop for determining F_x , we shall assume, for section CD,

$$\begin{aligned} I &= 0.0491(D^4 - d^4) = 0.0491(\overline{2.0^4} - \overline{1.281^4}) \\ &= 0.653 \text{ in.}^4. \end{aligned}$$

If $E = 27.4 \times 10^6 \text{ psi}$,

$$F_x = \frac{27.4 \times 10^6 (0.653)(0.0527)}{1284} = 734 \text{ lb.}$$

The maximum moment occurs at points C and D, and is

$$M = F_x(BC) = 734 \times 5 = 3670 \text{ lb-in.}$$

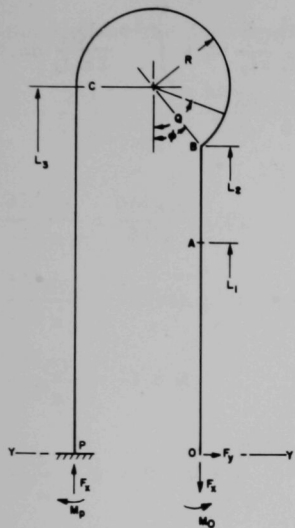
To determine stress we shall use I_2 of tubing at point C:

$$I_2 = 0.0491(\overline{1.25^4} - \overline{0.75^4}) = 0.104 \text{ in.}^2.$$

The bending stress, assuming no correction factors, is

$$\sigma_b = \frac{Mr}{I_2} = \frac{3670(0.625)}{0.104} = 22,055 \text{ lb/in.}^2.$$

As a second approximation, we shall use method of strain energy of bending to determine moments and forces acting on loop. We shall assume a model symmetrical about the Y-Y axis as shown in the accompanying figure. Because of symmetry, we need only consider one half in our analysis. Again, point P may be considered fixed and point O free to move to the right with $F_y = 0$. At O, the moment M_O and tensile force F_x act as shown.



We follow the procedure in S. Timoshenko, Strength of Materials, Part II, Second Ed., D. Van Nostrand Co., Inc., New York (1944), p. 79. The strain energy of bending is given by

$$U = \int_0^L \frac{M^2 ds}{2EI},$$

where the integration is carried out over the entire length L of the loop. Timoshenko shows that the deflection of the point at which the load acts in the direction of the load is

$$\delta = \frac{\partial U}{\partial F_x}.$$

Likewise, he shows that the angular displacement of a point due to a moment acting at the point is

$$\theta = \frac{\partial U}{\partial M_O}.$$

In the case in question, because of symmetry, there is no rotation at point O. Consequently,

$$\theta = 0 = \frac{\partial U}{\partial M_O}.$$

The load F_x and the moment M_O will also have to be such as to give a deformation equal to one half the differential expansion between the Inconel and the stainless steel:

$$\delta = \frac{\Delta X}{2} = \frac{0.0527}{2} = 0.02635 \text{ in.} = \frac{\partial U}{\partial F_x}.$$

An example very similar to ours is given in J. H. Faupel, Engineering Design, John Wiley & Sons, Inc., New York (1964), p. 863. If we consider

only bending and disregard longitudinal and shearing forces, the total energy of half loop is

$$U = \int_0^{L_1} \frac{M_{OA}^2}{2E_1I_1} dx + \int_0^{L_2} \frac{M_{AB}^2}{2E_2I_2} dx + \int_{\varphi}^{\frac{3\pi}{2}} \frac{M_{BC}^2}{2E_2kI_2} d\varphi + \int_0^{L_3} \frac{M_{CP}^2}{2E_2I_3} dx.$$

Now

$$M_{OA} = M_O;$$

$$M_{AB} = M_O;$$

$$M_{BC} = M_O - F_x R (\sin \varphi - \sin \varphi);$$

$$M_{CP} = M_O - F_x R \left(\sin \varphi - \sin \frac{3\pi}{2} \right);$$

$$\frac{\partial U}{\partial M_O} = 0 = \int_0^{L_1} \frac{M_{OA}}{E_1I_1} \frac{\partial M_{OA}}{\partial M_O} dx + \dots + \dots;$$

$$\frac{\partial M_{OA}}{\partial M_O} = \frac{\partial M_{AB}}{\partial M_O} = \frac{\partial M_{BC}}{\partial M_O} = \frac{\partial M_{CP}}{\partial M_O} = 1.$$

Since $\sin \varphi = 0.6$,

$$M_{CP} = M_O - 1.6 F_x R$$

and

$$\begin{aligned} \frac{\partial U}{\partial M_O} = 0 &= \int_0^{L_1} \frac{M_O}{E_1I_1} dx + \int_{L_1}^{L_2} \frac{M_O}{E_2I_2} dx + \int_{\varphi}^{\frac{3\pi}{2}} \frac{M_O - F_x R (\sin \varphi - \sin \varphi)}{E_2kI_2} R d\varphi \\ &+ \int_0^{L_3} \frac{M_O - 1.6 F_x R}{E_2I_3} dx \\ &= \frac{M_O L_1}{E_1I_1} + \frac{M_O (L_2 - L_1)}{E_2I_2} + \frac{(M_O - 1.6 F_x R) L_3}{E_2I_3} + \frac{M_O R}{E_2kI_2} \left(\frac{3\pi}{2} - \varphi \right) \\ &- \frac{F_x R^2}{E_2kI_2} \left[\sin \varphi (\psi - \varphi) + \cos \frac{3\pi}{2} - \cos \varphi \right], \end{aligned}$$

where k is a flexibility factor used to modify I when the integration is taken over a curved section. Since $\varphi = 0.643$,

$$0 = \frac{M_O L_1}{E_1 I_1} + \frac{M_O (L_2 - L_1)}{E_2 I_2} + \frac{M_O L_3}{E_2 I_3} - \frac{1.6 F_x R L_3}{E_2 I_3} + \frac{4.067 M_O R}{E_2 k I_2} - \frac{1.64 F_x R^2}{E_2 k I_2}.$$

Solving for the deflection, we obtain

$$\delta = \frac{\partial U}{\partial F_x} = \int_0^{L_1} \frac{M_{OA}}{E_1 I_1} \frac{\partial M_{OA}}{\partial F_x} dx + \dots ;$$

$$\frac{\partial M_{OA}}{\partial F_x} = \frac{\partial M_{AB}}{\partial F_x} = 0;$$

$$\frac{\partial M_{BC}}{\partial F_x} = -R(\sin \varphi - \sin \varphi);$$

$$\frac{\partial M_{CP}}{\partial F_x} = -1.6 R;$$

$$\begin{aligned} \frac{\partial U}{\partial F_x} = \delta = 0 + 0 + \int_{\varphi}^{\frac{3\pi}{2}} \frac{[M_O - F_x R(\sin \varphi - \sin \varphi)][-R(\sin \varphi - \sin \varphi)] R d\varphi}{E_2 k I_2} \\ + \int_0^{L_3} \frac{(M_O - 1.6 F_x R)(-1.6 R) dx}{E_2 I_3}; \end{aligned}$$

$$\delta = \frac{2.778 F_x R^3}{E_2 k I_2} - \frac{1.64 M_O R^2}{E_2 k I_2} - \frac{1.6 R M_O L_3}{E_2 I_3} + \frac{2.56 F_x R^2 L_3}{E_2 I_3} = 0.02635.$$

In accordance with the piping code,

$$k = 1.65/h$$

where $h = tR/r^2$, t the wall thickness, R the bend radius, and r the median radius of tube. Then,

$$h = \frac{(0.25)(2.5)}{(0.5)^2} = 2.5$$

and

$$k = \frac{1.65}{2.5} = 0.66.$$

According to the code, k may not be less than 1.

Tabulating various values:

$$E_1 = 31 \times 10^6 \text{ psi};$$

$$R = 2.5 \text{ in.};$$

$$E_2 = 27.4 \times 10^6 \text{ psi};$$

$$I_1 = 0.0491(\overline{1.25^4} - \overline{1.05^4}) = 0.060 \text{ in.}^4;$$

$$L_1 = 12.937 \text{ in.};$$

$$I_2 = 0.0491(\overline{1.25^4} - \overline{0.75^4}) = 0.104 \text{ in.}^4;$$

$$L_2 = 19.437 \text{ in.};$$

$$I_3 = 0.0491(\overline{2.0^4} - \overline{1.281^4}) = 0.653 \text{ in.}^4.$$

$$L_3 = 23.937 \text{ in.};$$

Evaluating both equations, we get

$$0 = 14.031 \times 10^{-6} M_O - 8.502 \times 10^{-6} F_X;$$

$$0.02635 = -8.502 \times 10^{-6} M_O + 34.850 \times 10^{-6} F_X.$$

Solving these simultaneously, we get

$$F_X = 887 \text{ lb}$$

and

$$M_O = 538 \text{ lb-in.}$$

By inspection, the maximum moment occurs at point C and is

$$M_{\max} = M_O - 4 F_X = 538 - 4(887) = -3010 \text{ lb-in.}$$

The bending stress is

$$\sigma_b = \frac{Mr_O}{iI},$$

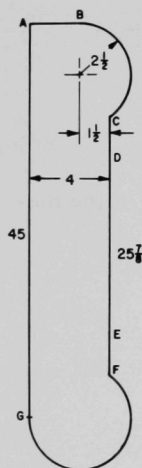
where

$$i = 0.9/h^{2/3} = 0.9/1.83 = 0.492.$$

According to the piping code, i must have unit value, so that

$$\sigma_b = \frac{3010(0.625)}{0.104} = 18,088 \text{ lb/in.}^2.$$

Because the actual loop is not quite as flexible as indicated by the previous model, we consider the complete loop. We shall show that equilibrium is reached without any damaging stress. For this analysis, the model shown in the accompanying figure will be used.



The differential expansion of segment EGAD and DE is equilibrated by the following:

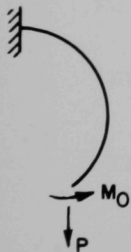
1. Elongation of DE, CD, and EF.
2. Compression of AG.
3. Deformation of BC and FG.
4. Displacement of points D and E due to rotation of AG.

The approach we use is essentially the same as in the previous model. For a continuum to exist, $\Sigma \delta$ must equal the differential expansion and $\Sigma \theta$ must equal zero.

Following is a tabulation of properties of the segments:

Segment	OD x ID	φ -Area, in. ²	L or ($\psi - \varphi$)	I_p	$E_c \times 10^{-6}$, psi	$\alpha \times 10^6$, °F ⁻¹	$E_h \times 10^6$
AB	Assume Rigid		2.5		∞	10.29	
BC	$1\frac{1}{4} \times 3/4$	0.785	($\pi - 0.643$)	0.104	27.4	10.29	22.8
CD	$1\frac{1}{4} \times 3/4$	0.785	6.125	0.104	27.4	10.29	22.8
DE	1.25×1.05	0.361	25.875	0.060	31.0	8.1	25.0
EF	$1\frac{1}{4} \times 3/4$	0.785	6.500	0.104	27.4	10.29	22.8
FG	$1\frac{1}{4} \times 3/4$	0.785	($3\pi/2 - 0.643$)	0.104	27.4	10.29	22.8
GA	$2 \times 1\frac{9}{32}$	1.852	45	0.653	27.4	10.29	22.8

Let us now look at each segment to determine deformations and rotations. Due to the differential expansion, a vertical load P and a moment M_O are induced in the system at points D and E. We consider a free-body diagram of each segment.



Consider segment BC, as in the accompanying figure. We have*

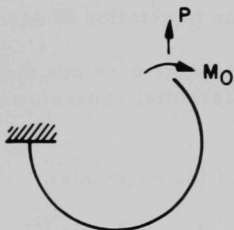
$$\begin{aligned} \delta_{BC} &= \frac{P(2.5)^3}{27.4 \times 10^6} \frac{(0.228)}{(0.104)} + \frac{M_O(2.5)^2}{27.4 \times 10^6(0.104)} (0.301) \\ &= 1.250 \times 10^{-6} P + 0.660 \times 10^{-6} M. \end{aligned}$$

We can safely assume that deformations and rotations are small, and therefore P and M_O load segment BC as shown.

*See Part 3 of this appendix for derivation.

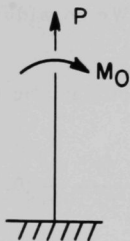
$$\begin{aligned}\theta_{BC} &= \frac{P(2.5)^2(0.301)}{27.4 \times 10^6(0.104)} - \frac{M_O(2.5)(2.498)}{27.4 \times 10^6(0.104)} \\ &= 0.660 \times 10^{-6} P + 2.192 \times 10^{-6} M_O.\end{aligned}$$

For segment FG,



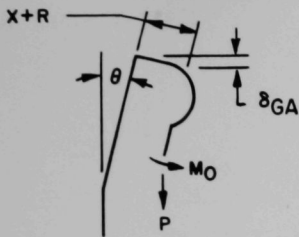
$$\begin{aligned}\delta_{FG} &= \frac{P(2.5)^3}{27.4 \times 10^6(0.104)} (2.778) - \frac{M_O(2.5)^2}{27.4 \times 10^6(0.104)} (1.640) \\ &= 15.232 \times 10^{-6} P - 3.597 \times 10^{-6} M_O; \\ \theta_{FG} &= \frac{-P(2.5)^2(1.640)}{27.4 \times 10^6(0.104)} + \frac{M_O(2.5)(4.067)}{27.4 \times 10^6(0.104)} \\ &= -3.597 \times 10^{-6} P + 3.568 \times 10^{-6} M_O.\end{aligned}$$

For segment DE,



$$\begin{aligned}\delta_{DE} &= \frac{PL}{AE} = \frac{P(25.875)}{0.361 \times 31.0 \times 10^6} \\ &= 2.312 \times 10^{-6} P; \\ \theta_{DE} &= \frac{M_O L}{EI} = \frac{M_O(25.875)}{31.0 \times 10^6(0.060)} \\ &= 13.911 \times 10^{-6} M_O.\end{aligned}$$

For segment GA, the deformation of point C (and D) due to rotation is given by (see accompanying figure)



$$\delta_{GA} = (X+R) \theta_{GA}; \quad X+R = 4;$$

$$\begin{aligned} \theta_{GA} &= \frac{ML}{EI} = \frac{(4P - M_O)L}{EI} = \frac{(4P)45}{27.4 \times 10^6(0.653)} \\ &\quad - \frac{45 M_O}{27.4 \times 10^6(0.653)} \\ &= 10.060 \times 10^{-6} P - 2.515 \times 10^{-6} M_O. \end{aligned}$$

Accordingly,

$$\delta_{GA} = 40.241 \times 10^{-6} P - 10.060 \times 10^{-6} M_O.$$

By compression,

$$\delta_{GA} = \frac{PL}{AE} = \frac{45P}{1.852 \times 27.4 \times 10^6} = 0.887 \times 10^{-6} P.$$

For segment CD,

$$\delta_{CD} = \frac{PL}{AE} = \frac{6.125P}{0.785 \times 27.4 \times 10^6} = 0.285 \times 10^{-6} P;$$

$$\theta_{CD} = \frac{M_O L}{EI} = \frac{6.125 M_O}{27.4 \times 10^6(0.104)} = 2.149 \times 10^{-6} M_O.$$

For segment EF,

$$\delta_{EF} = \frac{PL}{AE} = \frac{P \times 6.500}{0.785 \times 27.4 \times 10^6} = 0.302 \times 10^{-6} P;$$

$$\theta_{EF} = \frac{M_O L}{EI} = \frac{M_O \times 6.500}{27.4 \times 10^6(0.104)} = 2.281 \times 10^{-6} M_O.$$

A tabulation of these values follows:

Segment	$\delta_i \times 10^6$	$\theta_i \times 10^6$
GA	41.128 P - 10.060 M_O	10.060 P - 2.515 M_O
BC	1.250 P + 0.660 M_O	-0.660 P - 2.192 M_O
FG	15.232 P - 3.597 M_O	+3.597 P - 3.568 M_O
DE	2.312 P	- 13.911 M_O
CD	0.285 P	- 2.149 M_O
EF	0.302 P	- 2.281 M_O
Σ	60.509 P - 12.997 M_O	12.997 P - 26.616 M_O

The differential expansion between the Inconel and the stainless is

$$\begin{aligned}\delta &= (\alpha_1 - \alpha_2) \Delta T L \\ &= (10.29 - 8.1) \times 10^{-6} (1000 - 70) 25.875 \\ &= 0.0527.\end{aligned}$$

Further,

$$\Sigma \delta_i = \delta = 0.0527 = 60.509 P - 12.997 M_O$$

and

$$\Sigma \theta = 0 = 12.997 P - 26.616 M_O.$$

Solving these simultaneous equations, we find

$$P = 973 \text{ lb}; M_O = 475 \text{ lb-in.}$$

The critical section is at point G, where the moment is

$$\begin{aligned}M &= 4 P - M_O \\ &= 4(973) - 475 = 3417 \text{ lb-in.}\end{aligned}$$

The bending stress is

$$S_b = i \frac{M_c}{I} = 1 \times \frac{3417(0.625)}{(0.104)} = 20,535 \text{ lb/in.}^2.$$

The total stress is obtained by adding longitudinal stress due to internal pressure, the direct stress due to P, and the bending stress:

$$\begin{aligned}S &= 6000 \times \frac{0.785(0.75)^2}{0.785} - \frac{975}{0.785} + 20,535 \\ &= 3375 - 1242 + 20,535 \\ &= 22,668 \text{ lb/in.}^2.\end{aligned}$$

The allowable expansion stress range is

$$S_A = f(1.25 S_C + 0.25 S_H).$$

When the number of stress cycles is less than 7000, $f = 1$.

From Table N-421 in ASME Boiler and Pressure Vessel Code, $S_C = 20,000 \text{ lb/in.}^2$. No ratings are given for temperatures in excess of 800°F . We could extrapolate some value by a comparison with those given in Table N-424.

	Temperature, $^\circ\text{F}$		
	100	800	1,000
N-424	30,000	16,400	15,700
Y.S., lb/in.^2			
N-421	20,000	15,600	?
Design Stress, lb/in.^2			

A value of $14,000 \text{ lb/in.}^2$ would seem to be a conservative value when we compare the difference between yield and design stress at 800°F . Then

$$S_A = 1(1.25 \times 20,000 + 0.25 \times 14,000) = 28,500 \text{ lb/in.}^2.$$

This is considerably more than the $20,535 \text{ lb/in.}^2$ calculated for $S_E (= S_b)$, indicating stress limitations are being met.

We will calculate stress values giving full consideration to hot-value moduli of elasticity and cold springing. With cold springing of 0.020 , the effective δ is $0.0527 - 0.020 = 0.0327$. Using 22.8×10^6 for Type 316 stainless steel at 1000°F and 25×10^6 for Inconel at 1000°F , the solution of $\Sigma\delta$ and $\Sigma\theta$ becomes

$$0.0327 = 72.805 \times 10^{-6} P - 15.619 \times 10^{-6} M_O$$

$$0 = 15.619 \times 10^{-6} P - 32.518 \times 10^{-6} M_O,$$

whence

$$P = 500 \text{ lb-in.};$$

$$M_O = 240 \text{ lb-in.};$$

$$\sigma_b = \frac{(4 \times 500 - 240)(0.625)}{(0.104)} = 10,577 \text{ lb/in.}^2;$$

$$\sigma = S_L - \frac{P}{A} + \sigma_b = 3375 - 637 + 10,577 = 13,315 \text{ lb/in.}^2.$$

The fact that this is below the yield stress must explain why no permanent set was encountered in actual operation of the loop.

We shall now check the Mark-IIA design, where segments BC and FG are fabricated from $1\frac{3}{8}$ -in.-OD by 3/4-in.-ID tubing.

The moment of inertia is

$$I = 0.0491(\overline{1.375^4} - \overline{0.750^4}) = 0.160 \text{ in.}^4.$$

When this value for I is used for segments BC and FG, the equations for $\Sigma\delta$ and $\Sigma\theta$ become

$$0.0527 = 54.74 P - 11.969 M_O; \quad 0 = 11.969 P - 24.603 M_O.$$

The solution of these equations results in the following values:

$$P = 1077 \text{ lb; } M_O = 524 \text{ lb-in.}$$

The corresponding maximum bending stress is

$$S_b = \frac{[4(1077) - 524](0.687)}{0.160} = 16,247 \text{ lb/in.}^2.$$

This value is below the allowable S_A and is safe.

2. Dump Tank Loop for TREAT Mark IIB

Consider the piping loop to be represented by Fig. B.1. The loop is considered to be two-dimensional, although the actual loop is three-dimensional. Solutions for the two-dimensional loop provide a somewhat conservative estimate, since the three-dimensional loop is more flexible. The overflow tube was neglected because, due to its small moment of inertia and length, it will be quite flexible. The method of strain energy of bending is used to determine moments and forces acting on the loop. Points H and O are considered to be fixed, and member AI (the dump tank) is considered to be perfectly rigid. Equations are obtained for the vertical deflections (δ) and angular displacements (θ) of piping segments I and II. Combining these equations with the equation for thermal expansion and the fact that forces, moments, and angular displacements are equal at the point shown in the exploded view of segment AB (Fig. B.1), the forces and the moments can be found.

Following the procedure in Timoshenko, the strain energy of bending is

$$U = \int_0^L \frac{M^2}{2EI} ds,$$

where the integration is carried out over the entire length of the two segments (I and II).

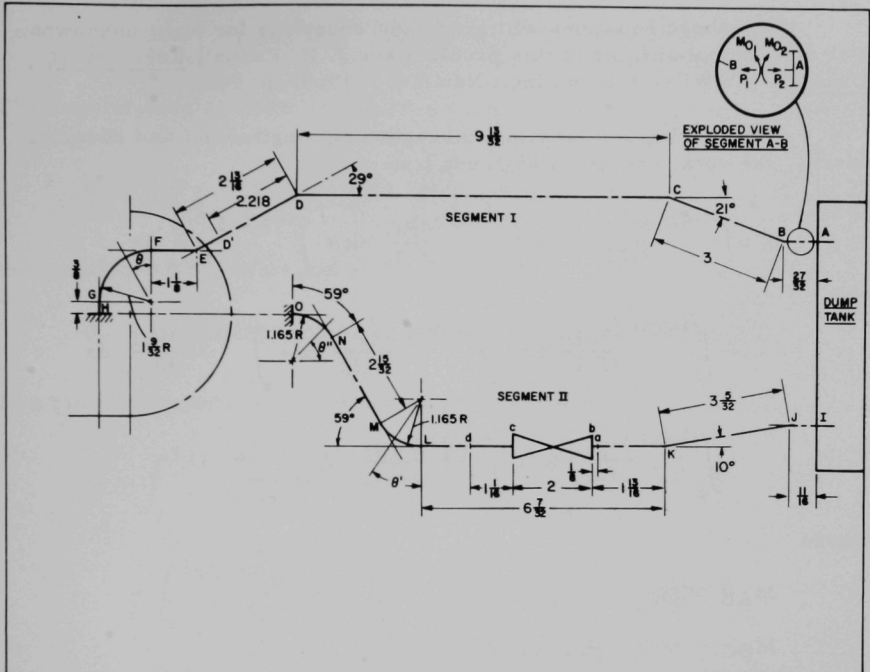


Fig. B.1. Piping Schematic Diagram

Timoshenko shows that the deflection of the point at which the load acts in the direction of the load is

$$\delta = \frac{\partial U}{\partial P}.$$

Likewise, he shows that the angular displacement of a point due to a moment acting at the point is

$$\theta = \frac{\partial U}{\partial M_O}.$$

The net thermal expansion is given by

$$\Delta = \delta_1 + \delta_2.$$

Also,

$$P_1 = P_2; M_{O_1} = M_{O_2}; \theta_1 = \theta_2.$$

The above equations will give eight equations for eight unknowns. For an example similar to this problem see J. H. Faupel, Engineering Design, John Wiley & Sons, Inc., New York (1964), p. 863.

Considering only bending, disregarding longitudinal and shearing forces, the total energy of segment I is

$$\begin{aligned}
 U = & \int_0^{LAB} \frac{M_{AB}^2}{2E_2I_a} dx + \int_0^{LBC} \frac{M_{BC}^2}{2E_2I_a} dx + \int_0^{LCD} \frac{M_{CD}^2}{2E_2I_a} dx \\
 & + \int_0^{LDD'} \frac{M_{DD'}^2}{2E_2I_a} dx + \int_0^{LD'E} \frac{M_{D'E}^2}{2E_2I_a} dx + \int_0^{LEF} \frac{M_{EF}^2}{2E_2I_a} dx \\
 & + \int_0^{LFG} \frac{M_{FG}^2}{2E_2I_a} dx + \int_0^{LGH} \frac{M_{GH}^2}{2E_2I_a} dx,
 \end{aligned}$$

where

$$M_{AB} = M_{O_1};$$

$$M_{BC} = M_{O_1} - P_1 x \sin 21^\circ;$$

$$M_{CD} = M_{O_1} - P_1(3 \sin 21^\circ);$$

$$M_{DD'} = M_{O_1} - P_1(2.218 - x) \sin 29^\circ;$$

$$M_{D'E} = M_{O_1} + P_1 x \sin 29^\circ;$$

$$M_{EF} = M_{O_1} + P_1(2.813 - 2.218) \sin 29^\circ;$$

$$M_{FG} = M_{O_1} + P_1[(2.813 - 2.218) \sin 29^\circ + 1\frac{9}{32}(1 - \cos \theta)],$$

$$0 < \theta < 90^\circ;$$

$$M_{GH} = M_{O_1} + P_1[(2.813 - 2.218) \sin 29^\circ + 1\frac{9}{32} + x].$$

Thus, the deflection in segment I is

$$\delta_1 = \frac{\partial U}{\partial P_1} = \int_0^{LAB} \frac{M_{AB}}{E_2I_a} \frac{\partial M_{AB}}{\partial P_1} dx + \dots$$

Substituting respective moments and solving yield

$$\delta_1 = \frac{1}{E_2 I_a} \left[-11.848 M_{O_1} + 14.155 P_1 + 1.518 \frac{M_{O_1}}{K_1} + 1.137 \frac{P_1}{K_1} \right].$$

The angular displacement in segment I is

$$\theta_1 = \frac{\partial U}{\partial M_{O_1}} = \int_0^{L_{AB}} \frac{M_{AB}}{E_2 I_a} \frac{\partial M_{AB}}{\partial M_{O_1}} dx + \dots$$

Substituting the moments and solving yield

$$\theta_1 = \frac{1}{E_2 I_a} \left[17.563 M_{O_1} - 11.848 P_1 + 2.013 \frac{M_{O_1}}{K_1} + 1.518 \frac{P_1}{K_1} \right].$$

In a similar manner, the total energy of segment II is

$$\begin{aligned} U = & \int_0^{L_{IJ}} \frac{M_{IJ}^2}{2E_1 I_a} dx + \int_0^{L_{JK}} \frac{M_{JK}^2}{2E_1 I_a} dx + \int_0^{L_{Ka}} \frac{M_{KL}^2}{2E_1 I_a} dx \\ & + \int_0^{L_{ab}} \frac{M_{KL}^2}{2E_1 I_c} dx + \int_0^{L_{bc}} \frac{M_{KL}^2}{2E_1 I_d} dx + \int_0^{L_{cd}} \frac{M_{KL}^2}{2E_1 I_c} dx \\ & + \int_0^{L_{dL}} \frac{M_{KL}^2}{2E_1 I_b} dx + \int_0^{L_{LM}} \frac{M_{LM}^2}{2E_1 k_2 I_b} dx + \int_0^{L_{MN}} \frac{M_{MN}^2}{2E_4 I_b} dx \\ & + \int_0^{L_{NO}} \frac{M_{NO}^2}{2E_3 k_3 I_b} dx, \end{aligned}$$

where

$$M_{IJ} = M_{O_2} + P_2 \left(4\frac{5}{8} \right)$$

$$M_{JK} = M_{O_2} + P_2 \left(4\frac{5}{8} \right) + Px \sin 10^\circ$$

$$M_{KL} = M_{O_2} + P_2 \left(4\frac{5}{8} + 3\frac{5}{32} \sin 10^\circ \right)$$

$$M_{LM} = M_{O_2} + P_2 \left[\left(4\frac{5}{8} + 3\frac{5}{32} \sin 10^\circ \right) - 1.165(1 - \cos \theta') \right], \quad 0 < \theta' < 59^\circ$$

$$M_{MN} = M_{O_2} + P_2 \left[\left(4\frac{5}{8} + 3\frac{5}{32} \sin 10^\circ \right) - 1.165(1 - \cos \theta') - x \sin 59^\circ \right]$$

$$M_{NO} = M_{O_2} + P_2 \left[\left(4\frac{5}{8} + 3\frac{5}{32} \sin 10^\circ \right) - 1.165(1 - \cos \theta') \right]$$

$$- 2\frac{15}{32} \sin 59^\circ - 1.165(\sin \theta'' - \sin 31^\circ)], \quad 31^\circ < \theta < 90^\circ.$$

Thus, the deflection in segment II is

$$\delta_2 = \frac{\partial U}{\partial P_2} = \int_0^{L_{IJ}} \frac{M_{IJ}}{E_1 I_a} \frac{\partial M_{IJ}}{\partial P_1} dx + \dots$$

Substituting respective moments and solving yield

$$\begin{aligned} \delta_2 = & \frac{1}{E_1 I_a} (27.372 M_{O_2} + 135.696 P_2) + \frac{1}{E_1 I_b} (6.951 M_{O_2} + 35.960 P_2) \\ & + \frac{1}{E_1 I_c} (6.143 M_{O_2} + 31.778 P_2) + \frac{1}{E_1 I_d} (10.346 M_{O_2} + 53.522 P_2) \\ & + \frac{1}{E_1 I_b} \left(5.972 \frac{M_{O_2}}{k_2} + 29.761 \frac{P_2}{k_2} \right) + \frac{1}{E_4 I_b} (8.820 M_{O_2} + 32.173 P_2) \\ & + \frac{1}{E_3 I_b} \left(4.849 \frac{M_{O_2}}{k_3} + 5.339 \frac{P_2}{k_3} \right). \end{aligned}$$

The angular displacement in segment II is

$$\theta_2 = \frac{\partial U}{\partial M_{O_2}} = \int_0^{L_{IJ}} \frac{M_{IJ}}{E_1 I_a} \frac{\partial M_{IJ}}{\partial M_{O_2}} dx + \dots$$

Substituting respective moments and solving yield

$$\begin{aligned} \theta_2 = & \frac{1}{E_1 I_a} (5.531 M_{O_2} + 27.372 P_2) + \frac{1}{E_1 I_b} (1.344 M_{O_2} + 6.951 P_2) \\ & + \frac{1}{E_1 I_c} (1.188 M_{O_2} + 6.143 P_2) + \frac{1}{E_1 I_d} (2.000 M_{O_2} + 10.346 P_2) \\ & + \frac{1}{E_1 I_b} \left(1.200 \frac{M_{O_2}}{k_2} + 5.807 \frac{P_2}{k_2} \right) + \frac{1}{E_4 I_b} (2.492 M_{O_2} + 8.821 P_2) \\ & + \frac{1}{E_3 I_b} \left(1.200 \frac{M_{O_2}}{k_3} + 2.523 \frac{P_2}{k_3} \right). \end{aligned}$$

The equations for the deflections and angular displacements will be used along with the information for thermal expansion, etc., to determine the forces and moments, and, hence, the maximum stresses in segments I and II for two different temperatures.

Case 1

- a) Segment I is at 400°F.
- b) Segment II is at various temperatures:
 - i. Segment LJKLM is at 125°F;
 - ii. Segment MN is at $(900 + 125)/2 = 513^\circ\text{F}$;
 - iii. Segment NO is at 900°F.

By using the values for moments of inertia, flexibility, and moduli of elasticity in the appendix, the equations for the deflection and angular displacements become

$$\delta_1 = -4.539 \times 10^{-5} M_{O_1} + 6.719 \times 10^{-5} P_1; \quad (1)$$

$$\theta_1 = 8.601 \times 10^{-5} M_{O_1} - 4.539 \times 10^{-5} P_1; \quad (2)$$

$$\delta_2 = 18.259 \times 10^{-5} M_{O_2} + 85.478 \times 10^{-5} P_2; \quad (3)$$

$$\theta_2 = 3.838 \times 10^{-5} M_{O_2} + 17.790 \times 10^{-5} P_2. \quad (4)$$

Also,

$$P_1 = P_2 = P; \quad (5)$$

$$M_{O_1} = M_{O_2} = M_O; \quad (6)$$

$$\theta_1 = \theta_2 = \theta. \quad (7)$$

The thermal expansion is given by

$$\Delta = \alpha_2 L_{AH_X} \Delta T_{AH} - (\alpha_1 L_{IJ_X} \Delta T_{IJ} + \alpha_4 L_{MN_X} \Delta T_{MN} + \alpha_3 L_{NO_X} \Delta T_{NO}) = \delta_1 + \delta_2,$$

where

$$L_{AH_X} = 18 \text{ in.}; \quad L_{IJ_X} = 11.063 \text{ in.};$$

$$L_{MN_X} = 1.156 \text{ in.}; \quad L_{NO_X} = 1.031 \text{ in.};$$

$$\Delta T_{AH} = 400 - 70 = 330^\circ\text{F}; \quad \Delta T_{IJ} = 125 - 70 = 55^\circ\text{F};$$

$$\Delta T_{MN} = 513 - 70 = 443^\circ\text{F}; \quad \Delta T_{NO} = 900 - 70 = 830^\circ\text{F}.$$

Thus, the value for the thermal expansion is

$$\Delta = \delta_1 + \delta_2 = 0.0377 \text{ in.} \quad (8)$$

Simultaneous solution of Eqs. 1-8 for P and M_O yields

$$P = 24.1 \text{ lb}; M_O = 113.0 \text{ lb-in.}$$

Consider the stresses due to bending moments:

i. Maximum stress in segment I occurs at point H. At this point,

$$\begin{aligned}\sigma_b &= \text{bending stress} = \frac{M_H d_0/2}{I_a} \\ &= \frac{\left\{ M_O + P \left[(2.813 - 2.218) \sin 29^\circ + 1\frac{9}{32} + 3/8 \right] \right\} d_0/2}{I_a} \\ &= \frac{[113.0 + (24.1)(1.945)] 0.675/2}{8.621 \times 10^{-3}} = 6260 \text{ lb/in.}^2.\end{aligned}$$

ii. Maximum stress in segment II occurs in segment KL at the points where the moments of inertia are a minimum:

$$\begin{aligned}\sigma_b &= \frac{M_{KL} d_0/2}{I_a} = \frac{\left[M_O + P \left(4\frac{5}{8} + 3\frac{5}{32} \sin 10^\circ \right) \right] 0.675/2}{8.621 \times 10^{-3}} \\ &= \frac{[113.0 + (24.1)(5.173)] 0.675/2}{8.621 \times 10^{-3}} = 9306 \text{ lb/in.}^2.\end{aligned}$$

iii. The stress at point O is given by

$$\begin{aligned}\sigma_b &= \frac{M_{NO} \text{ (for } \theta'' = 90^\circ) d/2}{I_b} = \frac{M_O + P(3.072 - 1.165 \sin \theta'') 0.840/2}{20.082 \times 10^{-3}} \\ &= \frac{113.0 + (24.1)(3.072 - 1.165)(0.840/2)}{20.082 \times 10^{-3}} = 3325 \text{ lb/in.}^2.\end{aligned}$$

Consider stresses due to the force P acting in tension, compression, or shear.

i. At point H,

$$\sigma_s = \frac{P}{A_s} = \frac{24.1}{0.2173} = 111 \text{ lb/in.}^2,$$

where A is the cross-sectional area.*

ii. In segment KL (at smallest area),

$$\sigma_T = \frac{P}{A_T} = \frac{24.1}{0.2173} = 111 \text{ lb/in.}^2.$$

iii. At point O,

$$\sigma_T = \frac{P}{A_T} = \frac{24.1}{0.320} = 76 \text{ lb/in.}^2.$$

Consider the total stresses

i. At point H (conservatively adding),

$$\sigma_H = \sigma_b + \sigma_s = 6260 + 111$$

$$= 6370 \text{ lb/in.}^2.$$

ii. In segment KL (conservatively adding),

$$\sigma_{KL} = \sigma_b + \sigma_T = 9306 + 111$$

$$= 9407 \text{ lb/in.}^2.$$

iii. At point O (conservatively adding),

$$\sigma_O = \sigma_b + \sigma_T = 3325 + 76$$

$$= 3401 \text{ lb/in.}^2.$$

Case 2

a) Segment I is at 900°F.

b) Segment II is at various temperatures:

i. Segment LJKLM is at 125°F;

ii. Segment MN is at $(900 + 125)/2 = 513^\circ\text{F}$;

iii. Segment NO is at 900°F.

Proceeding as in Case 1, the governing equations will be

$$\delta_1 = -5.165 \times 10^{-5} M_{O_1} + 7.646 \times 10^{-5} P_1; \quad (9)$$

$$\theta_1 = 9.787 \times 10^{-5} M_{O_1} - 5.165 \times 10^{-5} P_1; \quad (10)$$

$$\delta_2 = 18.259 \times 10^{-5} M_{O_2} + 85.478 \times 10^{-5} P_2; \quad (11)$$

$$\theta_2 = 3.838 \times 10^{-5} M_{O_2} + 17.790 \times 10^{-5} P_2; \quad (12)$$

$$P_1 = P_2 = P; \quad (13)$$

$$M_{O_1} = M_{O_2} = M_O; \quad (14)$$

$$\theta_1 = \theta_2 = \theta; \quad (15)$$

and

$$\Delta = \delta_1 + \delta_2 = 0.13249 \text{ in.} \quad (16)$$

Simultaneous solution of Eqs. 9-16 for P and M_O yields

$$P = 93.0 \text{ lb}; \quad M_O = 359.0 \text{ lb-in.}$$

Consider the stresses due to bending moments:

i. Maximum stress in segment I occurs at point H. At this point,

$$\begin{aligned} \sigma_b &= \text{bending stress} = \frac{M_H d_0 / 2}{I_a} \\ &= \frac{\{M_O + P[(2.813 - 2.218) \sin 29^\circ + \frac{1^9}{32} + 3/8]\} d_0 / 2}{I_a} \\ &= \frac{[359.0 + (93.0)(1.945)] 0.675 / 2}{8.621 \times 10^{-3}} = 21,135 \text{ lb/in.}^2. \end{aligned}$$

ii. Maximum stress in segment II occurs in segment KL at the points where the moments of inertia are a minimum:

$$\begin{aligned} \sigma_b &= \frac{M_{KL} d_0 / 2}{I_a} = \frac{[M_O + P(4\frac{5}{8} + 3\frac{5}{32} \sin 10^\circ)] 0.675 / 2}{8.621 \times 10^{-3}} \\ &= \frac{[359.0 + 93.0(4\frac{5}{8} + 3\frac{5}{32} \sin 10^\circ)] 0.675 / 2}{8.621 \times 10^{-3}} = 32,889 \text{ lb/in.}^2. \end{aligned}$$

iii. For stress at point O,

$$\begin{aligned} \sigma_b &= \frac{M_{NO} (\text{for } \theta'' = 90^\circ) d / 2}{I_b} = \frac{M_O + P(3.072 - 1.165 \sin \theta'') 0.840 / 2}{20.082 \times 10^{-3}} \\ &= \frac{359.0 + 93.0(3.072 - 1.165) 0.840 / 2}{20.082 \times 10^{-3}} = 11,219 \text{ lb/in.}^2. \end{aligned}$$

Stresses due to the force P , acting in tension, compression, or shear are:

- i. At point H,

$$\sigma_s = \frac{P}{A_s} = \frac{93.0}{0.2173} = 428 \text{ lb/in.}^2,$$

where A is the cross-sectional area.

- ii. In segment KL (at smallest area),

$$\sigma_T = \frac{P}{A_T} = \frac{93.0}{0.2173} = 428 \text{ lb/in.}^2.$$

- iii. At point O,

$$\sigma_T = \frac{P}{A_T} = \frac{93.0}{0.320} = 291 \text{ lb/in.}^2.$$

For the total stresses,

- i. At point H (conservatively adding),

$$\sigma_H = \sigma_b + \sigma_s = 21,135 + 428$$

$$= 21,563 \text{ lb/in.}^2.$$

- ii. In segment KL (conservatively adding),

$$\sigma_{KL} = \sigma_b + \sigma_T = 32,889 + 428$$

$$= 33,317 \text{ lb/in.}^2.$$

- iii. At point O (conservatively adding),

$$\sigma_O = \sigma_b + \sigma_T = 11,219 + 291$$

$$= 11,510 \text{ lb/in.}^2.$$

3. Basic Data for Dump Tank Loop for TREAT Mark IIB

a. Moduli of Elasticity, E [from Steels for Elevated Temperature Service, United States Steel Corporation publication ADUSS 43-1089 (1966)].

(1) At 125°F, $E_1 = 28.2 \times 10^6 \text{ lb/in.}^2$.

(2) At 400°F, $E_2 = 26.4 \times 10^6 \text{ lb/in.}^2$.

(3) At 900°F, $E_3 = 23.2 \times 10^6 \text{ lb/in.}^2$.

(4) At $(900 + 125)/2 = 513^\circ\text{F}$, $E_4 = 25.7 \times 10^6 \text{ lb/in.}^2$.

b. Moments of Inertia, I

(1) For 3/8 Schedule 80 pipe,

$$I_a = 0.0491(d_0^4 - d_1^4) = 0.0491(0.675^4 - 0.423^4) = 8.621 \times 10^{-3} \text{ in.}^4.$$

(2) For 1/2 Schedule 80 pipe,

$$I_b = 0.0491(d_0^4 - d_1^4) = 0.0491(0.840^4 - 0.546^4) = 20.082 \times 10^{-3} \text{ in.}^4.$$

(3) For inlet and outlet of dump valve,

$$I_c = 0.0491[(3/4)^4 - (3/8)^4] = 14.56 \times 10^{-3} \text{ in.}^4.$$

(4) For dump valve,

$$I_d = 0.0491(1.09375^4 - 0.78125^4) = 51.94 \times 10^{-3} \text{ in.}^4.$$

c. Flexibility Factors, k

(1) For segment GF,

$$k_1 = \frac{1.65}{tR/r_m^2} = \frac{1.65 r_m^2}{tR},$$

where

$$r_m = 0.268 \text{ in.}$$

$$t = 0.126 \text{ in.}$$

$$R = 1\frac{9}{32} \text{ in.} = 1.281 \text{ in.}$$

Accordingly,

$$k_1 = \frac{(1.65)(0.268)^2}{(0.126)(1.281)} = 0.735.$$

Per piping code, k may not be less than 1. Hence, we take

$$k_1 = 1.$$

(2) For segment LM,

$$k_2 = \frac{1.65 r_m^2}{tR},$$

where

$$r_m = 0.342 \text{ in.}$$

$$t = 0.147 \text{ in.}$$

$$R = 1.165 \text{ in.}$$

Accordingly,

$$k_2 = \frac{(1.65)(0.342)^2}{(0.147)(1.165)} = 1.126.$$

(3) For segment NO,

$$k_3 = \frac{1.65 r_m^2}{tR},$$

where

$$r_m = 0.342 \text{ in.}$$

$$t = 0.147 \text{ in.}$$

$$R = 1.165 \text{ in.}$$

Accordingly,

$$k_3 = \frac{(1.65)(0.342)^2}{(0.147)(1.165)} = 1.126.$$

d. Coefficients of Thermal Expansion, α [from Piping Design and Engineering, second edition, published by Grinnel Company, Inc., (1967)].

$$(1) \text{ At } 125^\circ\text{F}, \alpha_1 = 9.23 \times 10^{-6} \text{ (in./in.)}/^\circ\text{F.}$$

$$(2) \text{ At } 400^\circ\text{F}, \alpha_2 = 9.59 \times 10^{-6} \text{ (in./in.)}/^\circ\text{F.}$$

$$(3) \text{ At } 900^\circ\text{F}, \alpha_3 = 10.16 \times 10^{-6} \text{ (in./in.)}/^\circ\text{F.}$$

$$(4) \text{ At } (900 + 125)/2 = 513^\circ\text{F}, \alpha_4 = 9.72 \times 10^{-6} \text{ (in./in.)}/^\circ\text{F.}$$

REFERENCES

1. E. S. Sowa and J. C. Heap, *The Development of a Small Integral Loop for In-pile Fuel-failure Studies in the Presence of Flowing Sodium*, Trans. Amer. Nucl. Soc. 8(2), 559 (1965).
2. L. E. Robinson, R. T. Purviance, and F. L. Willis, "Modification of the TREAT Integral Sodium Loops," *Reactor Physics Division Annual Report: July 1, 1964 to June 30, 1965*, ANL-7110, pp. 268-274 (Dec 1965).
3. ASME Boiler and Pressure Vessel Code, 1965 Edition.
4. ASME Boiler and Pressure Vessel Code, 1968 Edition, Sect. III, "Nuclear Vessels."
5. L. R. Blake, *Conduction and Induction Pumps for Liquid Metals*, Proc. Inst. Elec. Eng. 104A, 49 (1956).
6. E. Cambillard and B. Schwab, *Annulus Electromagnetic Pumps; Construction and Testing. Theory and Comparison with Experimental Results*, CEA-R-2523 (1964).
7. L. E. Robinson and R. D. Carlson, *The Development of Pumps for Use in Fast-reactor-safety Integral-loop Experiments*, ANL-7369 (Apr 1968).
8. R. D. Carlson and R. J. Schiltz, *Power Transformer for Use in Highly Radioactive Environments*, TID-14021 (Aug 1961).
9. L. E. Robinson and R. T. Purviance, *Pressure Transducers for TREAT Sodium Loops*, ANL-7107 (June 1969).
10. R. J. Roark, *Formulas for Stress and Strain*, 4th Edition, McGraw-Hill Book Co., Inc., New York (1967).
11. L. E. Robinson, "Design of the Mark-II Integral Transient Reactor Test (TREAT) Facility Sodium Loop," *Reactor Physics Division Annual Report: July 1, 1965 to June 30, 1966*, ANL-7210, pp. 245-250 (Dec 1966).

ARGONNE NATIONAL LAB WEST



3 4444 00008293 3

X

